PHYSICAL REVIEW E VOLUME 53, NUMBER 2 FEBRUARY 1996

Lyapunov instability in a system of hard disks in equilibrium and nonequilibrium steady states

Ch. Dellago and H. A. Posch
Institut für Experimentalphysik, Universität Wien, Boltzmanngasse 5, A-1090 Wien, Austria

W. G. Hoover
Department of Applied Science, University of California at Davis–Livermore and Lawrence Livermore National Laboratory, Livermore, California 94 551-7808
(Received 10 July 1995)

We present a generalization of Benettin's classical algorithm for the calculation of full Lyapunov spectra to the case of dynamical systems where the smooth streaming is interrupted by a differentiable map at discrete times. With this formalism we derive the transformation rules for the offset vectors in tangent space for a system of hard particles in equilibrium and nonequilibrium steady states. In particular, we study the color conductivity of a system of hard disks carrying color charges subjected to an external color field. Full Lyapunov spectra are obtained numerically for equilibrium systems of 64 and 144 hard disks. Furthermore, the maximum Lyapunov exponent and the Kolmogorov-Sinai entropy are studied over a wide range of densities. Both mimic the collision rate very well. In the low density regime the maximum Lyapunov exponent is found to follow the relation $\lambda_1 \propto -\rho\ln\rho$, as conjectured by Krylov. Full Lyapunov spectra are also reported for nonequilibrium steady-state systems of 64 hard disks, which carry color charges and are externally perturbed by an applied color field. The simulations cover a wide range of densities and fields. From a careful study of small three- and four-particle systems the validity of the conjugate pairing rule is established numerically with an error less than 0.1%. Also the number of vanishing Lyapunov exponents due to the conserved quantities—center of mass, linear momentum, and kinetic energy—is discussed in some detail.

PACS number(s): 05.45.+b, 02.70.Ns, 05.20.−y, 05.70.Ln

I. MOTIVATION

Since the pioneering work of Alder and Wainwright [1,2], in which they laid down the foundations of the molecular dynamics method, a huge amount of work has been done on systems of elastic hard disks or spheres. A wealth of highly interesting phenomena has been discovered in this apparently simple model, one of the most fundamental being that the hypothesis of local molecular chaos is not strictly valid [3]. Stated in more exact terms, the velocity autocorrelation function of the particles does not decay exponentially, but follows a power law for long times, which means that the system loses memory of past states very slowly. In spite of this, well behaved transport coefficients are found in molecular dynamics simulation of nonequilibrium steady-state systems, even in two dimensions and in the thermodynamic limit [4]. Since the transport coefficients of a many-body system are intimately related to its Lyapunov spectrum [5,6], it seems plausible that this peculiarity of two-dimensional hard-disk fluids should be reflected also in their Lyapunov spectrum. Another property of hard disks and hard spheres, which turns out to have a major impact on the Lyapunov instability of the system, is the solid-fluid phase transition first discovered by Alder and Wainwright [7,8].

Hard-sphere systems belong to a minority of models for which rigorous mathematical results exist. It has been proved that they are unstable in the sense of Lyapunov and exhibit C-system behavior, which means that they are ergodic and mixing [9–11]. But no attempts at the numerical computation of Lyapunov spectra have been undertaken up to now. For many-body systems this property has been explored only for models with smooth interaction potentials [12]. The reason for this disparity lies in the availability of practical and accurate numerical algorithms for the calculation of Lyapunov spectra for smooth dynamical systems, and the lack of such methods for systems involving hard-core interactions. Nevertheless, due to their simple dynamics hard-sphere systems should provide new insight into the microsopic processes determining the mechanical instability of many-body sytems.

In this paper we demonstrate how the classic algorithm of Benettin *et al.* [13,14], already used for the calculation of Lyapunov spectra of fluids in equilibrium and nonequilibrium steady states with phase space dimension ranging from 2 to 400 [15] for the evaluation of full spectra, and to 129 600 for the maximum exponent [4], can be generalized to the case of hard elastic interactions. In Sec. II the theoretical background and necessary definitions are provided. In Sec. III algorithms for the computation of full Lyapunov spectra are derived for a number of models of increasing complexity which involve hard-disk collisions without or with an applied external force. In Sec. IV we study many-body systems of hard disks in equilibrium and nonequilibrium steady states and provide a numerical test for the validity of the conjugate pairing principle. We also show that due to subtle properties of the

 ©1996 The American Physical Society

algorithm concerning the conservation of momentum in the tangent space dynamics d Lyapunov exponents in a d-dimensional space may be negative instead of zero in contrast to naive expectation.

II. LYAPUNOV EXPONENTS

Typically, the many-body systems mentioned above have a strong sensitivity to initial conditions, which means that two phase points initially separated by a small distance in phase space tend to diverge exponentially. In this case the system is said to be chaotic. To state the problem in a more quantitative way, we consider a general L-dimensional smooth dynamical system

$$\dot{\mathbf{\Gamma}} = \mathbf{F}(\mathbf{\Gamma}), \tag{1}$$

where $\mathbf{\Gamma}$ is an L-dimensional vector in the phase space of the system. The integration of this coupled set of ordinary differential equations gives the temporal evolution of the system, the so-called phase flow,

$$\mathbf{\Gamma}(t) = \Phi^t(\mathbf{\Gamma}(0)), \tag{2}$$

which will be assumed to be bounded. Let $\mathbf{\Gamma}(t)$ denote the reference trajectory, and $\mathbf{\Gamma}_s(t)$ a perturbed trajectory connected to $\mathbf{\Gamma}(t)$ by a parametrized path with parameter s such that $\lim_{s\to 0}\mathbf{\Gamma}_s(t) = \mathbf{\Gamma}(t)$. The associated tangent vector is defined by

$$\delta\mathbf{\Gamma}(t) = \lim_{s\to 0}\frac{\mathbf{\Gamma}_s(t) - \mathbf{\Gamma}(t)}{s}. \tag{3}$$

Its equation of motion is obtained by linearizing (1),

$$\delta\dot{\mathbf{\Gamma}} = \mathbf{D}(\mathbf{\Gamma})\cdot\delta\mathbf{\Gamma}, \tag{4}$$

where $\mathbf{D}(\mathbf{\Gamma}) = \partial\mathbf{F}/\partial\mathbf{\Gamma}$ is the Jacobi matrix of the system. To avoid unnecessary notation we will not make the limit and the denominator of (3) explicit in the following and will refer to $\delta\mathbf{\Gamma}(t)$ as an infinitesimal vector separating neighboring orbits and describing the temporal evolution of an (infinitesimal) perturbation.

For chaotic systems this perturbation grows exponentially, which motivates the definition of the Lyapunov exponents of a trajectory for initial conditions $\mathbf{\Gamma}(0)$ and an initial displacement $\delta\mathbf{\Gamma}(0)$ as

$$\lambda(\mathbf{\Gamma}(0),\delta\mathbf{\Gamma}(0)) = \lim_{t\to\infty}\frac{1}{t}\ln\frac{|\delta\mathbf{\Gamma}(t)|}{|\delta\mathbf{\Gamma}(0)|}. \tag{5}$$

Oseledec's multiplicative ergodic theorem [16] states that for ergodic systems under very general assumptions λ exists and that there are L orthonormal initial vectors $\delta\mathbf{\Gamma}_l(0)$ yielding a set of L exponents $\{\lambda_l\}$, which is referred to as the Lyapunov spectrum of the system. The exponents are taken to be ordered, $\lambda_1 \geq \lambda_2 \geq \cdots \geq \lambda_L$. Since, according to Oseledec, the λ_l are independent of the metric and the initial condition, we can drop the argument $\mathbf{\Gamma}(0)$. Geometrically the Lyapunov exponents can be interpreted as the mean exponential growth rates of the principal axes of an infinitesimal ellipsoid surrounding a phase point and evolving according to (1). Thus the Lyapunov spectrum describes the stretching and contraction characteristics of the phase flow.

The Lyapunov exponents of the class of symplectic systems, to which our hard particles belong if in equilibrium, exhibit a Smale-pair symmetry, $\lambda_l + \lambda_{L+1-l} = 0$, for $l = 1,\ldots,L$. This symmetry reduces the numerical effort for the calculation of full Lyapunov spectra by a factor of 2, and can also be used as a check of the algorithm. Furthermore, for each quantity conserved by the equations of motion one Lyapunov exponent vanishes. In a d-dimensional equilibrium system of N hard particles and phase space dimension $L = 2dN$ the total momentum, the total (kinetic) energy, and the center of mass coordinates are conserved. Since also one exponent associated with a displacement in the flow direction equals zero, altogether $2d+2$ Lyapunov exponents vanish in this case.

Nonequilibrium steady-state systems cease to be symplectic and become dissipative. Nevertheless, the Smale-pairing symmetry is not totally lost for homogeneous systems for which conjugate pairs of exponents add up to a constant negative value [17]. The total sum of all Lyapunov exponents is negative and corresponds to irreversible entropy production [5]. Furthermore, it can be shown [18] that the sum of all Lyapunov exponents can be related to the respective macroscopic transport coefficients. The number of vanishing exponents due to the conserved quantities—center of mass, momentum, and kinetic energy—in the nonequilibrium case is a more subtle question which will be treated in detail in Sec. IV B.

The practical computation of Lyapunov spectra according to the classic algorithm of Benettin *et al.* [13] proceeds by simultaneously solving the original equations of motion (1) for the reference trajectory $\mathbf{\Gamma}(t)$ and the linear variational equations (4) for a complete set of offset vectors $\{\delta\mathbf{\Gamma}_l\}$. The difficulties associated with the choice of the generally unknown initial vectors $\delta\mathbf{\Gamma}_l(0)$ and the rounding-error effects of the computer are overcome by periodic reorthonormalization of the set of offset vectors, such that the Lyapunov exponents are obtained from the time averaged logarithms of the respective normalizing factors. For a more in-depth treatment of this algorithm the reader is referred to [13,14].

III. ALGORITHM AND MODELS

Whereas the classical method of Benettin *et al.* can be straightforwardly applied to differentiable dynamical systems, more refined methods are necessary to treat systems, which are, loosely speaking, hybrid models of ordinary differential equations and discrete maps. Recently [19,20] we calculated the Lyapunov exponents for the Sinai stadium billiard and for the Lorentz gas in equilibrium and nonequilibrium steady states by adapting the Benettin *et al.* algorithm to the case of elastic impulsive collisions. In this section we reformulate the problem in a more general way and derive a scheme for the calculation of Lyapunov spectra for such hybrid models.

Let us consider the autonomous set of L coupled ordinary differential equations (1) with initial conditions $\mathbf{\Gamma}(0)$, and let us assume that, in addition, the transformation

$$\mathbf{\Gamma}_f = \mathbf{M}(\mathbf{\Gamma}_i) \tag{6}$$

is applied at discrete times $\{\tau_1, \tau_2, \tau_3, \ldots\}$. The map $\mathbf{M}(\mathbf{\Gamma})$ is assumed to be differentiable with respect to the phase space variables. The subscripts i and f denote the initial and the final states of the map $\mathbf{M}$. In the time intervals $\tau_{i+1} - \tau_i$ the trajectory is determined by integrating Eq. (1), which yields the smooth flow Φ^t. The time evolution of the offset vectors is obtained by integrating Eq. (4). Taking into account also the singular mapping events at the times $\{\tau_i\}$, the whole time evolution in phase space and in tangent space can be written as

$$\begin{aligned}\mathbf{\Gamma}(t) &= \Phi^{t-\tau_n} \circ \mathbf{M} \circ \Phi^{\tau_n - \tau_{n-1}} \circ \cdots \circ \Phi^{\tau_2 - \tau_1} \\ &\quad \circ \mathbf{M} \circ \Phi^{\tau_1}\, \mathbf{\Gamma}(0), \end{aligned} \tag{7}$$

$$\delta\mathbf{\Gamma}(t) = \mathbf{L}^{t-\tau_n} \cdot \mathbf{S} \cdot \mathbf{L}^{\tau_n - \tau_{n-1}} \cdots \mathbf{L}^{\tau_2 - \tau_1} \cdot \mathbf{S} \cdot \mathbf{L}^{\tau_1} \cdot \delta\mathbf{\Gamma}(0), \tag{8}$$

where $\mathbf{L}$ is the propagator of $\delta\mathbf{\Gamma}$ in the smooth segments, and $\mathbf{S}$ is the map in tangent space corresponding to $\mathbf{M}$. The propagator $\mathbf{L}$ can be formally written as

$$\mathbf{L}^{t_2 - t_1} = \exp_+ \left\{ \int_{t_1}^{t_2} \mathbf{D}[\mathbf{\Gamma}(t')]\, dt' \right\}, \tag{9}$$

where $\exp_+$ denotes a time ordered exponential.

The effect of a single application of the map $\mathbf{S}$ on the offset vectors is schematically shown in Fig. 1. For simplicity the phase space is taken to be two dimensional. In the following this discrete event is called a *collision*, but we stress that our results are valid for all differentiable discrete maps, and not just for elastic impulsive collisions.

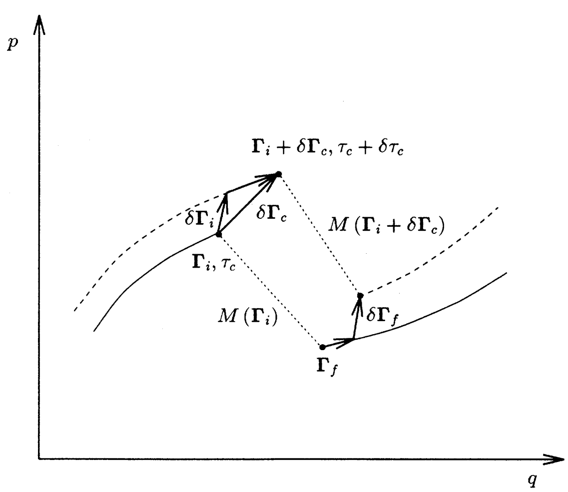

FIG. 1. Effect of the noncontinuous transformation $\mathbf{M}$ on the offset vectors in the tangent space of the system.

In Fig. 1 the reference trajectory is drawn as a solid line, whereas the satellite trajectory is represented by a broken line. For the reference trajectory the collision takes place at the phase point $\mathbf{\Gamma}_i$ and at the time τ_c and maps the phase space vector $\mathbf{\Gamma}_i$ into the vector $\mathbf{\Gamma}_f$. The satellite trajectory undergoes collision at a displaced point $\mathbf{\Gamma}_i + \delta\mathbf{\Gamma}_c$ and at a different time $\tau_c + \delta\tau_c$. We note that the time delay $\delta\tau_c$ can be positive as well as negative. As can be seen from Fig. 1 the offset vector $\delta\mathbf{\Gamma}_f$ immediately after the collision of both trajectories is given by

$$\delta\mathbf{\Gamma}_f = \mathbf{M}(\mathbf{\Gamma}_i + \delta\mathbf{\Gamma}_c) - [\mathbf{\Gamma}_f + \mathbf{F}(\mathbf{\Gamma}_f)\,\delta\tau_c], \tag{10}$$

where we have taken advantage of the short time approximation

$$\mathbf{\Gamma}(t + \delta t) = \mathbf{\Gamma}(t) + \mathbf{F}(\mathbf{\Gamma})\,\delta t. \tag{11}$$

Using the same linearization we obtain

$$\delta\mathbf{\Gamma}_c = \delta\mathbf{\Gamma}_i + \mathbf{F}(\mathbf{\Gamma}_i)\,\delta\tau_c. \tag{12}$$

Insertion of this result into (10) and application of the linear approximation

$$\mathbf{M}(\mathbf{\Gamma} + \delta\mathbf{\Gamma}) = \mathbf{M}(\mathbf{\Gamma}) + \frac{\partial \mathbf{M}}{\partial \mathbf{\Gamma}} \cdot \delta\mathbf{\Gamma} \tag{13}$$

finally yields an expression for $\delta\mathbf{\Gamma}_f$ as a function of the phase space vector and the offset vector before the collision:

$$\delta\mathbf{\Gamma}_f = \frac{\partial \mathbf{M}}{\partial \mathbf{\Gamma}} \cdot \delta\mathbf{\Gamma}_i + \left[\frac{\partial \mathbf{M}}{\partial \mathbf{\Gamma}} \cdot \mathbf{F}(\mathbf{\Gamma}_i) - \mathbf{F}(\mathbf{M}(\mathbf{\Gamma}_i)) \right] \delta\tau_c. \tag{14}$$

We note that the time delay $\delta\tau_c$ is a function of $\mathbf{\Gamma}_i$ and $\delta\mathbf{\Gamma}_i$. This equation, obtained from a linear approximation in time *and* in phase space, is our point of departure for all subsequent calculations. We stress that it gives the exact linear tranformation rules for the offset vectors due to a discrete mapping. The ingredients necessary for the application of Eq. (14) are the equations of motion given by the vector $\mathbf{F}(\mathbf{\Gamma})$, the map $\mathbf{M}(\mathbf{\Gamma})$, and its derivative $\partial\mathbf{M}/\partial\mathbf{\Gamma}$. As a first example for the application of Eq. (14) we rederive the transformation rules for the offset vectors of two model systems, which were recently deduced by us from purely geometrical considerations [19,20]. Then we apply (14) to derive the offset-vector transformation rules for a hard-sphere system carrying color charges both in equilibrium and in the presence of an external field.

A. Collision of a two-dimensional point particle with a flat surface

The simplest system is given by a two-dimensional point particle of mass m colliding with a flat surface, on which it is elastically reflected. One can find this case in two-dimensional billards such as the stadium billiard [19]. The phase vector is

$$\mathbf{\Gamma} = \begin{pmatrix} \mathbf{q} \\ \mathbf{p} \end{pmatrix}, \tag{15}$$

where $\mathbf{q}$ and $\mathbf{p}$ are the position and the momentum vectors of the particle, respectively. Since the particle moves force-free between collisions, the equations of motion are given by

$$\dot{\mathbf{\Gamma}} = \begin{pmatrix} \dot{\mathbf{q}} \\ \dot{\mathbf{p}} \end{pmatrix} = \begin{pmatrix} \mathbf{p}/m \\ \mathbf{0} \end{pmatrix}. \tag{16}$$

The particle is elastically reflected, which means that the transformation $\mathbf{M}$ leaves the position $\mathbf{q}$ and the momentum component parallel to the surface unchanged and changes the sign of the perpendicular component of the momentum:

$$\mathbf{\Gamma}_f = \mathbf{M}(\mathbf{\Gamma}_i) = \begin{pmatrix} \mathbf{q}_i \\ \mathbf{p}_i - 2(\mathbf{p}_i \cdot \mathbf{n})\,\mathbf{n} \end{pmatrix}, \tag{17}$$

where $\mathbf{n}$ is the unit vector perpendicular to the surface at the collision point. The collision of the satellite trajectory is delayed with respect to the reference trajectory by

$$\delta\tau_c = -\frac{(\delta\mathbf{q}_i \cdot \mathbf{n})}{(\mathbf{p}_i/m \cdot \mathbf{n})}, \tag{18}$$

which is simply the satellite-particle separation perpendicular to the surface divided by its normal velocity. For the Jacobian matrix associated with the map $\mathbf{M}$ we obtain

$$\frac{\partial \mathbf{M}}{\partial \mathbf{\Gamma}} = \begin{pmatrix} \mathbf{1} & \mathbf{0} \\ \mathbf{0} & (\mathbf{1} - 2\mathbf{n} \otimes \mathbf{n}) \end{pmatrix}, \tag{19}$$

where $\mathbf{0}, \mathbf{1}$, and $\mathbf{n} \otimes \mathbf{n}$ are 2×2 submatrices. The notation $\mathbf{d} \otimes \mathbf{e}$ implies a tensorial product of two vectors $\mathbf{d}$ and $\mathbf{e}$. Insertion of these expressions into (14) finally yields

$$\delta\mathbf{\Gamma}_f = \begin{pmatrix} \delta\mathbf{q}_i - 2(\delta\mathbf{q}_i \cdot \mathbf{n})\,\mathbf{n} \\ \delta\mathbf{p}_i - 2(\delta\mathbf{p}_i \cdot \mathbf{n})\,\mathbf{n} \end{pmatrix}, \tag{20}$$

i.e., both the position and the momentum components of the offset vector are reflected on the surface. We note that the reflection rule for the position components is automatically obtained from Eq. (14) and is a consequence of the time difference $\delta\tau_c$ between the collisions of the reference and the satellite trajectory. Geometrical arguments lead to identical results [19].

B. Collision of a two-dimensional point particle with a curved surface

Next we consider the collision of a point particle with a curved surface. This type of collision occurs, for example, in billiards with curved walls, and in the so-called Lorentz gas [19]. Again the phase vector, the equations of motion, the collision transformation rule and the time delay are given by Eqs. (15), (16), (17), and (18), respectively. But, due to the curvature of the surface, the normal vector $\mathbf{n}$ is now a function of the collision point. This must be taken into account for the derivation of the collision map $\mathbf{M}$:

$$\frac{\partial \mathbf{M}}{\partial \mathbf{\Gamma}} = \begin{pmatrix} \mathbf{1} & \mathbf{0} \\ \mathbf{A} & \mathbf{B} \end{pmatrix}, \tag{21}$$

where

$$\mathbf{A} = \frac{\partial \mathbf{p}_f}{\partial \mathbf{q}_i} = -2\,[\mathbf{n} \otimes \mathbf{p}_i + (\mathbf{p}_i \cdot \mathbf{n})\,\mathbf{1}] \cdot \frac{\partial \mathbf{n}}{\partial \mathbf{q}_i} \tag{22}$$

and

$$\mathbf{B} = \frac{\partial \mathbf{p}_f}{\partial \mathbf{p}_i} = \mathbf{1} - 2\mathbf{n} \otimes \mathbf{n}. \tag{23}$$

Thus the operator $\mathbf{B}$ corresponds simply to a reflection at the collision point. $\partial\mathbf{n}/\partial\mathbf{q}$ is the matrix of the derivatives of the normal vector $\mathbf{n}$ with respect to the position of the collision point. Equation (14) finally yields

$$\delta\mathbf{q}_f = \delta\mathbf{q}_i - 2(\delta\mathbf{q}_i \cdot \mathbf{n})\,\mathbf{n}, \tag{24}$$

$$\delta\mathbf{p}_f = \mathbf{B} \cdot \delta\mathbf{p}_i + \mathbf{A} \cdot \delta\mathbf{q}_c, \tag{25}$$

where $\delta\mathbf{q}_c = \delta\mathbf{q}_i + (\mathbf{p}_i/m)\delta\tau_c$ is the difference vector in configuration space between the collision points of the reference and the satellite trajectory. Thus the exact transformation rule for the offset vectors becomes

$$\delta\mathbf{\Gamma}_f = \begin{pmatrix} \delta\mathbf{q}_i - 2(\delta\mathbf{q}_i \cdot \mathbf{n})\,\mathbf{n} \\ \delta\mathbf{p}_i - 2(\delta\mathbf{p}_i \cdot \mathbf{n})\,\mathbf{n} - 2(\,(\mathbf{p}_i \cdot \delta\mathbf{n})\,\mathbf{n} + (\mathbf{p}_i \cdot \mathbf{n})\,\delta\mathbf{n}) \end{pmatrix}. \tag{26}$$

Here, $\delta\mathbf{n} = \partial\mathbf{n}/\partial\mathbf{q}_i \cdot \delta\mathbf{q}_c$ is the variation of $\mathbf{n}$ due to the displacement $\delta\mathbf{q}_c$. We observe that the additional term $\mathbf{A} \cdot \delta\mathbf{q}_c$ appearing in (25) is a consequence of the curvature of the collision surface and is orthogonal to the final momentum $\mathbf{p}_f$ as can be seen by direct calculation. For a flat surface $\delta\mathbf{n}$ vanishes and Eq. (20) is recovered.

We now express the tranformation rules (26) in terms of the curvature of the collision surface, to make contact with previous work [19]. Since $\mathbf{n}$ is a unit vector, $\delta\mathbf{n}$ can be viewed as an infinitesimal rotation and is there-

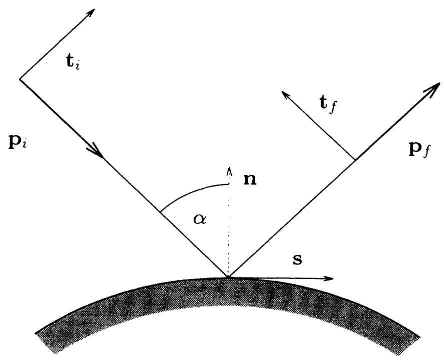

FIG. 2. Geometry of the collision of a point particle with a curved surface.

fore orthogonal to $\mathbf{n}$. Using the curvature κ_R, defined as the rate of change of the tangent vector orientation with growing distance from the collision point, we write $\delta\mathbf{n} = \kappa_R \delta s\, \mathbf{s}$. Here, δs is the displacement on the surface, and $\mathbf{s}$ is the tangent unit vector at the collision point and orthogonal to $\mathbf{n}$. We introduce the unit vectors $\mathbf{t}_i$ and $\mathbf{t}_f$ orthogonal to the vectors $\mathbf{p}_i$ and $\mathbf{p}_f$, respectively, as depicted in Fig. 2. Since $(\mathbf{p}_i \cdot \mathbf{s})\,\mathbf{n} + (\mathbf{p}_i \cdot \mathbf{n})\,\mathbf{s} = |\mathbf{p}_i|\; \mathbf{t}_f$ and $\delta s = (\delta \mathbf{q}_i \cdot \mathbf{t}_i)\,/\cos\alpha$, where α is the incidence angle of the particle, the complete transformation rule for the offset vector $\delta\mathbf{\Gamma}_i$ may be written as

$$\delta\mathbf{\Gamma}_f = \begin{pmatrix} \delta\mathbf{q}_i - 2\,(\delta\mathbf{q}_i \cdot \mathbf{n})\,\mathbf{n} \\ \delta\mathbf{p}_i - 2\,(\delta\mathbf{p}_i \cdot \mathbf{n})\,\mathbf{n} - 2\kappa_R \frac{(\delta\mathbf{q}_i \cdot \mathbf{t}_i)}{\cos\alpha}\,|\mathbf{p}_i|\;\mathbf{t}_f \end{pmatrix} . \quad (27)$$

This expression is identical to that found in Ref. [19]. If Eq. (27) is applied to circular scatterers such as in the Lorentz gas and in the stadium billiard, the curvature $\kappa_R = \pm 1/R$, depending on whether the collision takes place on the outer or the inner side of the circle.

C. The driven Lorentz gas

As one of the simplest models for transport in deterministic systems the driven Lorentz gas has been the object of several recent studies [20–22]. In this model a two-dimensional point particle with mass m is moving through an array of circular scatterers, on which it is elastically reflected. In addition, the particle is subjected to an external homogeneous field $\mathbf{E}$. Furthermore, to enforce a nonequilibrium steady state a Gaussian thermostat is coupled to the system. Between collisions with the scatterers the particle evolves according to the motion equations

$$\dot{\mathbf{\Gamma}} = \begin{pmatrix} \dot{\mathbf{q}} \\ \dot{\mathbf{p}} \end{pmatrix} = \begin{pmatrix} \mathbf{p}/m \\ \mathbf{E} - \zeta\mathbf{p} \end{pmatrix} , \quad (28)$$

where the thermostat variable is chosen to keep the kinetic energy of the moving particle constant:

$$\zeta = (\mathbf{E}\cdot\mathbf{p})\,/\,(\mathbf{p}\cdot\mathbf{p}) . \quad (29)$$

In collisions with a scatterer the momentum component perpendicular to the surface of the scatterer changes sign, while the parallel momentum component, as well as the position of the particle, remains unchanged by the collision. This transformation is again described by (17), where the unit vector $\mathbf{n}$ points into the direction from the center of the scatterer to the collision point. Since also the Jacobian of the collision map $\mathbf{M}$ as well as the configurational part of the equations of motion is identical to the case treated before, the transformation rule for the configuration components is given by Eq. (24). To take the effect of the external field and the thermostat on the offset vector $\delta\mathbf{\Gamma}$ into account, we write down the momentum part of the transformation rule (14):

$$\begin{aligned} \delta\mathbf{p}_f = {} & \mathbf{B}\cdot\delta\mathbf{p}_i + \mathbf{A}\cdot\delta\mathbf{q}_c \\ & + \{\mathbf{B}\cdot[\mathbf{E} - \zeta(\mathbf{p}_i)\mathbf{p}_i] \\ & - [\mathbf{E} - \zeta(\mathbf{p}_f)\mathbf{p}_f]\}\,\delta\tau_c, \end{aligned} \quad (30)$$

where the operators $\mathbf{A}$ and $\mathbf{B}$ and the time delay $\delta\tau_c$ are the same as in the previous section. The first two terms on the right-hand side of this equation are identical to the field-free case (26). However, due to the field an additional term emerges. Since the thermostat variable ζ changes by

$$\zeta\,(\mathbf{p}_f) - \zeta\,(\mathbf{p}_i) = -2\frac{(\mathbf{E}\cdot\mathbf{n})\,(\mathbf{p}_i\cdot\mathbf{n})}{\mathbf{p}_i^2} \quad (31)$$

due to the collision, we finally obtain

$$\delta\mathbf{p}_f = \mathbf{B}\cdot\delta\mathbf{p}_i + \mathbf{A}\cdot\delta\mathbf{q}_c - 2\delta\tau_c\,(\mathbf{E}\cdot\mathbf{n})\,(\mathbf{t}_f\cdot\mathbf{n})\,\mathbf{t}_f, \quad (32)$$

where $\mathbf{t}_f$ is the unit vector normal to $\mathbf{p}_f$ as before.

Since the kinetic energy $K = \mathbf{p}^2/2m$ is conserved, also $\delta K = \mathbf{p}\cdot\delta\mathbf{p}/m$ must be conserved by the collision. As can be checked by direct calculation, our transformation rules obey this condition.

We want to make contact with the results of Ref. [20],

$$\delta\mathbf{p}'' = |\mathbf{E}|\delta\tau_c\,[\sin(\theta_{in} - \varphi) + \sin(\theta_{out} - \varphi)]\,\mathbf{t}_f, \quad (33)$$

where θ_{in} and θ_{out} are the angles of orientation of the incoming and outgoing momenta, respectively, and φ determines the orientation of the field $\mathbf{E}$. $\delta\mathbf{p}''$ is the field-induced part of $\delta\mathbf{p}_f$. Since

$$\mathbf{E} = |\mathbf{E}| \begin{pmatrix} \cos\varphi \\ \sin\varphi \end{pmatrix} , \quad \mathbf{t}_i = \begin{pmatrix} -\sin\theta_{in} \\ \cos\theta_{in} \end{pmatrix} ,$$

and

$$bft_f = \begin{pmatrix} -\sin\theta_{out} \\ \cos\theta_{out} \end{pmatrix} , \quad (34)$$

and $\mathbf{t}_i + \mathbf{t}_f = 2\,(\mathbf{t}_f\cdot\mathbf{n})\,\mathbf{n}$, we get

$$\delta\mathbf{p}'' = -2\delta\tau_c\,(\mathbf{E}\cdot\mathbf{n})\,(\mathbf{t}_f\cdot\mathbf{n})\,\mathbf{t}_f, \quad (35)$$

which is identical to the last term of Eq. (32).

The full transformation can be summarized as

$$\delta\mathbf{\Gamma}_f = \begin{pmatrix} \delta\mathbf{q}_i - 2\left(\delta\mathbf{q}_i\cdot\mathbf{n}\right)\mathbf{n} \\ \delta\mathbf{p}_i - 2\left(\delta\mathbf{p}_i\cdot\mathbf{n}\right)\mathbf{n} - 2\frac{(\delta\mathbf{q}_i\cdot\mathbf{t}_i)}{R\cos\alpha}\left|\mathbf{p}_i\right|\mathbf{t}_f - 2\delta\tau_c\left(\mathbf{E}\cdot\mathbf{n}\right)\left(\mathbf{t}_f\cdot\mathbf{n}\right)\mathbf{t}_f \end{pmatrix}. \tag{36}$$

Thus the joint action of the field and the thermostat generates an additional term in the momentum-component tranformation rule.

D. Gas of N hard disks

Now we turn our attention to the calculation of the Lyapunov spectra for hard disks (two dimensional) and hard spheres (three dimensional). For simplicity we discuss only disks in the following, but all our considerations are also valid for hard spheres. Consider a system of N identical hard disks of diameter σ and mass m. The state of such a system is described by the $4N$-dimensional phase space vector $\mathbf{\Gamma} = \left(\mathbf{q}^1,\mathbf{q}^2,\ldots,\mathbf{q}^N,\mathbf{p}^1,\mathbf{p}^2,\ldots,\mathbf{p}^N\right)$, where $\mathbf{q}^j$ and $\mathbf{p}^j$ are the position and the momentum of the jth disk, respectively. In the times between collisions the disks stream according to

$$\begin{array}{rcl}\dot{\mathbf{q}}^j &=& \mathbf{p}^j/m \\ \dot{\mathbf{p}}^j &=& \mathbf{0}\end{array} \quad \text{for } j = 1,\ldots,N, \tag{37}$$

and the equations of motion for the offset vectors are

$$\begin{array}{rcl}\delta\dot{\mathbf{q}}^j &=& \delta\mathbf{p}^j/m \\ \delta\dot{\mathbf{p}}^j &=& \mathbf{0}\end{array} \quad \text{for } j = 1,\ldots,N. \tag{38}$$

The streaming is interrupted by impulsive elastic collisions. A transformation to relative and center-of-mass coordinates shows that a collision between the disks k and l leads to the following transformation in phase space:

$$\mathbf{q}_f^j = \mathbf{q}_i^j \quad \text{for } j = 1,\ldots,N, \tag{39}$$
$$\mathbf{p}_f^j = \mathbf{p}_i^j \quad \text{for } j \neq k,l, \tag{40}$$
$$\mathbf{p}_f^k = \mathbf{p}_i^k + (\mathbf{p}\cdot\mathbf{q})\,\mathbf{q}/\sigma^2, \tag{41}$$
$$\mathbf{p}_f^l = \mathbf{p}_i^l - (\mathbf{p}\cdot\mathbf{q})\,\mathbf{q}/\sigma^2, \tag{42}$$

where $\mathbf{q} = \mathbf{q}_i^l - \mathbf{q}_i^k$ and $\mathbf{p} = \mathbf{p}_i^l - \mathbf{p}_i^k$ are the relative position and momentum of the colliding disks k and l. The positions of all particles and the momenta of all the *other* particles not involved in the collision remain unaffected, while the momenta of the colliding particles suffer an instantaneous change. Again the collision of the disks k and l does not occur simultaneously for the reference trajectory and its satellite trajectory. The time delay $\delta\tau_c$ is given by the separation of the two trajectories along the vector $\mathbf{q}$ connecting the centers of the colliding particles, divided by the relative velocity in this direction,

$$\delta\tau_c = -\frac{(\delta\mathbf{q}\cdot\mathbf{q})}{(\mathbf{p}/m\cdot\mathbf{q})}, \tag{43}$$

where $\delta\mathbf{q} = \delta\mathbf{q}^l - \delta\mathbf{q}^k$. Next, we calculate the Jacobian for the collision matrix $\mathbf{M}$:

$$\frac{\partial\mathbf{M}}{\partial\mathbf{\Gamma}} = \begin{pmatrix}\mathbf{1} & \mathbf{0} \\ \mathbf{A} & \mathbf{B}\end{pmatrix}, \tag{44}$$

where $\mathbf{1}$ and $\mathbf{0}$ are the $2N\times 2N$ unit and zero matrices, respectively. The $2N\times 2N$ matrices $\mathbf{A} = (\mathbf{a}_{mn})$ and $\mathbf{B} = (\mathbf{b}_{mn})$ are composed of the 2×2 matrices $\mathbf{a}_{mn}$ and $\mathbf{b}_{mn}$ referring to the particle pair m,n for $m = 1,\ldots,N$ and $n = 1,\ldots,N$, which are defined by

$$\mathbf{a}_{mn} = \frac{\partial\mathbf{p}_f^m}{\partial\mathbf{q}_i^n} \quad\text{and}\quad \mathbf{b}_{mn} = \frac{\partial\mathbf{p}_f^m}{\partial\mathbf{p}_i^n}. \tag{45}$$

If k and l are the colliding particles one obtains from (41) and (42)

$$\mathbf{a}_{mn} = \mathbf{0} \quad\text{if}\quad (m,n)\notin\{(k,k),(k,l),(l,k),(l,l)\}, \tag{46}$$

$$\mathbf{a}_{kk} = \mathbf{a}_{ll} = -\frac{1}{\sigma^2}\left[\mathbf{q}\otimes\mathbf{p} + (\mathbf{q}\cdot\mathbf{p})\,\mathbf{1}\right], \tag{47}$$

$$\mathbf{a}_{kl} = \mathbf{a}_{lk} = \frac{1}{\sigma^2}\left[\mathbf{q}\otimes\mathbf{p} + (\mathbf{q}\cdot\mathbf{p})\,\mathbf{1}\right]. \tag{48}$$

The product $\mathbf{W} = \mathbf{A}\cdot\mathbf{U}$ of $\mathbf{A}$ with an arbitrary $2N$-dimensional vector $\mathbf{U}$ becomes

$$\mathbf{w}^j = \mathbf{0}\ \forall\ j\neq k,l, \tag{49}$$
$$\mathbf{w}^k = \mathbf{a}_{kk}\cdot\mathbf{u}^k + \mathbf{a}_{kl}\cdot\mathbf{u}^l = \tilde{\mathbf{a}}\cdot\left(\mathbf{u}^l - \mathbf{u}^k\right) = \tilde{\mathbf{a}}\cdot\mathbf{u}, \tag{50}$$
$$\mathbf{w}^l = \mathbf{a}_{lk}\cdot\mathbf{u}^k + \mathbf{a}_{ll}\cdot\mathbf{u}^l = \tilde{\mathbf{a}}\cdot\left(\mathbf{u}^k - \mathbf{u}^l\right) = -\tilde{\mathbf{a}}\cdot\mathbf{u}, \tag{51}$$

where $\tilde{\mathbf{a}} = \left[\mathbf{q}\otimes\mathbf{p} + (\mathbf{q}\cdot\mathbf{p})\,\mathbf{1}\right]/\sigma^2$ and $\mathbf{u} = \mathbf{u}^l - \mathbf{u}^k$. For the matrices $\mathbf{b}_{mn}$ we obtain

$$\mathbf{b}_{mn} = \mathbf{0} \quad\text{if}\quad m\neq n \quad\text{and}\quad (m,n)\notin\{(k,l),(l,k)\}, \tag{52}$$

$$\mathbf{b}_{mm} = \mathbf{1} \quad\text{if}\quad m\neq k \quad\text{and}\quad m\neq l, \tag{53}$$

$$\mathbf{b}_{kk} = \mathbf{b}_{ll} = \mathbf{1} - \frac{1}{\sigma^2}\mathbf{q}\otimes\mathbf{q}, \tag{54}$$

$$\mathbf{b}_{kl} = \mathbf{b}_{lk} = \frac{1}{\sigma^2}\mathbf{q}\otimes\mathbf{q}. \tag{55}$$

The product $\mathbf{V} = \mathbf{B}\cdot\mathbf{U}$ of $\mathbf{B}$ with an arbitrary $2N$-dimensional vector $\mathbf{U}$ reads

$$\mathbf{v}^j = \mathbf{u}^j \quad \forall\ j\neq k,l, \tag{56}$$
$$\mathbf{v}^k = \mathbf{b}_{kk}\cdot\mathbf{u}^k + \mathbf{b}_{kl}\cdot\mathbf{u}^l = \mathbf{u}^k + (\mathbf{u}\cdot\mathbf{q})\,\mathbf{q}/\sigma^2, \tag{57}$$
$$\mathbf{v}^l = \mathbf{b}_{lk}\cdot\mathbf{u}^k + \mathbf{b}_{ll}\cdot\mathbf{u}^l = \mathbf{u}^l - (\mathbf{u}\cdot\mathbf{q})\,\mathbf{q}/\sigma^2. \tag{58}$$

Thus the operator $\mathbf{B}$ corresponds to a specular reflection in relative coordinates of the components of $\mathbf{U}$ belonging to the colliding particles.

We are now able to apply Eq. (14) to the hard-disk system. First we determine the effect of the collision of particles k and l on the configuration components of the offset vector:

$$\delta \mathbf{q}_f^j = \delta \mathbf{q}_i^j + \left(\mathbf{p}_i^j/m - \mathbf{p}_f^j/m\right) \delta\tau_c. \tag{59}$$

For $j \neq k, l$ the momentum does not change in the collision, and we find

$$\delta \mathbf{q}_f^j = \delta \mathbf{q}_i^j \quad \text{if} \quad j \neq k, l. \tag{60}$$

For the components belonging to the colliding particles we obtain

$$\delta \mathbf{q}_f^k = \delta \mathbf{q}_i^k + \left(\mathbf{p}_i^k/m - \mathbf{p}_f^k/m\right) \delta\tau_c = \delta \mathbf{q}_i^k + (\delta\mathbf{q}\cdot\mathbf{q})\,\mathbf{q}/\sigma^2, \tag{61}$$

$$\delta \mathbf{q}_f^l = \delta \mathbf{q}_i^l + \left(\mathbf{p}_i^l/m - \mathbf{p}_f^l/m\right) \delta\tau_c = \delta \mathbf{q}_i^l - (\delta\mathbf{q}\cdot\mathbf{q})\,\mathbf{q}/\sigma^2, \tag{62}$$

where $\delta\mathbf{q} = \delta\mathbf{q}^l - \delta\mathbf{q}^k$. Applying the operators $\mathbf{A}$ and $\mathbf{B}$ we get the transformation rules for the momentum component of the offset vector,

$$\begin{aligned}\delta\mathbf{P}_f &= \mathbf{A}\cdot\delta\mathbf{Q}_i + \mathbf{B}\cdot\delta\mathbf{P}_i + (\mathbf{A}\cdot\mathbf{P}_i/m - \mathbf{0})\,\delta\tau_c \\ &= \mathbf{A}\cdot\delta\mathbf{Q}_c + \mathbf{B}\cdot\delta\mathbf{P}_i,\end{aligned} \tag{63}$$

where $\mathbf{Q} = (\mathbf{q}_1, \mathbf{q}_2, \ldots, \mathbf{q}_N)$ and $\mathbf{P} = (\mathbf{p}_1, \mathbf{p}_2, \ldots, \mathbf{p}_N)$ are the $2N$-dimensional vectors in configuration and momentum space, respectively. From Eqs. (49) and (56) it follows that

$$\delta\mathbf{p}_f^j = \delta\mathbf{p}_i^j \quad \text{if} \quad j \neq k, l, \tag{64}$$

$$\begin{aligned}\delta\mathbf{p}_f^k = \delta\mathbf{p}_i^k &+ (\delta\mathbf{p}\cdot\mathbf{q})\,\mathbf{q}/\sigma^2 \\ &+ \frac{1}{\sigma^2}\left[(\mathbf{p}\cdot\delta\mathbf{q}_c)\,\mathbf{q} + (\mathbf{p}\cdot\mathbf{q})\,\delta\mathbf{q}_c\right],\end{aligned} \tag{65}$$

$$\begin{aligned}\delta\mathbf{p}_f^l = \delta\mathbf{p}_i^l &- (\delta\mathbf{p}\cdot\mathbf{q})\,\mathbf{q}/\sigma^2 \\ &- \frac{1}{\sigma^2}\left[(\mathbf{p}\cdot\delta\mathbf{q}_c)\,\mathbf{q} + (\mathbf{p}\cdot\mathbf{q})\,\delta\mathbf{q}_c\right],\end{aligned} \tag{66}$$

where $\delta\mathbf{p} = \delta\mathbf{p}^l - \delta\mathbf{p}^k$. The displacement of the collision point $\delta\mathbf{q}_c$ is given by

$$\delta\mathbf{q}_c = \frac{(\delta\mathbf{q}_i\cdot\mathbf{t}_i)}{\cos\alpha}\mathbf{s}, \tag{67}$$

where α is the angle of incidence in relative coordinates and $\mathbf{s}$ is a unit vector normal to $\mathbf{q}$. Furthermore, we observe that $(\mathbf{p}\cdot\mathbf{s})\,\mathbf{q}/\sigma + (\mathbf{p}\cdot\mathbf{q}/\sigma)\,\mathbf{s} = |\mathbf{p}|\,\mathbf{t}_f$, where $\mathbf{t}_i$ and $\mathbf{t}_f$ are defined in the usual way in relative coordinates of the colliding particles. In this way we finally obtain the full and exact transformation rule for the offset vector:

$$\delta\mathbf{q}_f^j = \delta\mathbf{q}_i^j \quad \text{if} \quad j \neq k, l, \tag{68}$$

$$\delta\mathbf{q}_f^k = \delta\mathbf{q}_i^k + (\delta\mathbf{q}\cdot\mathbf{q})\,\mathbf{q}/\sigma^2, \tag{69}$$

$$\delta\mathbf{q}_f^l = \delta\mathbf{q}_i^l - (\delta\mathbf{q}\cdot\mathbf{q})\,\mathbf{q}/\sigma^2, \tag{70}$$

$$\delta\mathbf{p}_f^j = \delta\mathbf{p}_i^j \quad \text{if} \quad j \neq k, l, \tag{71}$$

$$\delta\mathbf{p}_f^k = \delta\mathbf{p}_i^k + (\delta\mathbf{p}\cdot\mathbf{q})\,\mathbf{q}/\sigma^2 + \frac{(\delta\mathbf{q}_i\cdot\mathbf{t}_i)}{\sigma\cos\alpha}|\mathbf{p}|\,\mathbf{t}_f, \tag{72}$$

$$\delta\mathbf{p}_f^l = \delta\mathbf{p}_i^l - (\delta\mathbf{p}\cdot\mathbf{q})\,\mathbf{q}/\sigma^2 - \frac{(\delta\mathbf{q}_i\cdot\mathbf{t}_i)}{\sigma\cos\alpha}|\mathbf{p}|\,\mathbf{t}_f. \tag{73}$$

If we combine these rules with the smooth equations of motion between collisions we can follow the exact time evolution of the offset vectors necessary to calculate the full Lyapunov spectrum.

E. Color conductivity in a gas of N hard disks

An interesting question is how is the Lyapunov spectrum of the hard-sphere system affected by an external perturbation? To investigate this question we consider the so-called "color conductivity" problem [5,17,18,23]. The system consists of N hard disks of equal mass m, which carry positive and negative color charges $c^j = \pm 1$. Charge neutrality is assumed: $\sum_{j=1}^{N} c^j = 0$. Through these charges the particles interact with a homogeneous external field $\mathbf{E}$ giving rise to the total interaction energy $-\sum_{j=1}^{N} c^j\left(\mathbf{E}\cdot\mathbf{q}^j\right)$. The interaction between the particles is not affected by their color charge. Since the charged particles continuously extract energy from the field, they are coupled to a Gaussian thermostat to achieve a steady nonequilibrium state. The equations of motion for the intercollisional trajectory segments become

$$\dot{\mathbf{q}}^j = \mathbf{p}^j/m, \tag{74}$$

$$\dot{\mathbf{p}}^j = c^j\mathbf{E} - \zeta\mathbf{p}^j, \tag{75}$$

$$\zeta = \frac{\sum_{j=1}^{N}\left(c^j\mathbf{E}\cdot\mathbf{p}^j\right)}{\sum_{j=1}^{N}\mathbf{p}^{j2}}. \tag{76}$$

The Gaussian thermostat keeps the kinetic energy $K = \sum_{j=1}^{N}(\mathbf{p}^j)^2/2m$—or even the total internal energy in the case of hard spheres—exactly constant. Because of charge neutrality also the total momentum of the system is conserved if it vanishes for $t = 0$. For simplicity we do not thermostat the system with respect to the local streaming velocity of the two particle species [17], but keep the total kinetic energy in the laboratory frame constant. As demonstrated by Posch and Hoover [18], this difference has no qualitative effect on the Lyapunov instability of the system.

From (74) and (75) the linearized equations of motion for the offset vectors between collisions are obtained:

$$\delta\dot{\mathbf{q}}^j = \delta\mathbf{p}^j/m, \tag{77}$$

$$\delta\dot{\mathbf{p}}^j = -\zeta\delta\mathbf{p}^j - \left(\frac{\sum_{k=1}^{N} \left(c^k\mathbf{E} - 2\mathbf{p}^k\zeta\right) \cdot \delta\mathbf{p}^k}{\sum_{k=1}^{N} (\mathbf{p}^k \cdot \mathbf{p}^k)} \right) \mathbf{p}^j. \quad (78)$$

Since with the constraint of conserved total energy the collision rules between particles do not change even in the presence of a driving field, the collision map $\mathbf{M}$ and also its derivatives $\partial\mathbf{M}/\partial\mathbf{\Gamma}$ are the same as in the case of unperturbed hard disks in equilibrium and need not be repeated here. Also the collision delay time $\delta\tau_c$ does not change. This implies that also the transformation rules for the configurational components of the offset vectors remain unchanged. However, the presence of the field and thermostat is responsible for an additional term $\delta\hat{\mathbf{p}}_f^j$ in the momentum tranformation rules. From (14) and the multiplication rules for the matrix $\mathbf{B}$ of the components belonging to the noncolliding particles we get

$$\delta\hat{\mathbf{p}}_f^j = [c^j\mathbf{E}-\zeta(\mathbf{P}_i)\mathbf{p}_i^j - c^j\mathbf{E}+\zeta(\mathbf{P}_f)\mathbf{p}_f^j]\delta\tau_c \quad \text{if } j \neq k,l. \quad (79)$$

The momenta of these particles do not change, i.e., $\mathbf{p}_i = \mathbf{p}_f$. This implies

$$\delta\hat{\mathbf{p}}_f^j = \Delta\zeta\mathbf{p}_i^j\delta\tau_c \quad \text{if } j \neq k,l, \quad (80)$$

where $\Delta\zeta \equiv \zeta(\mathbf{P}_f) - \zeta(\mathbf{P}_i)$ is the change of ζ due to the collision of particles k and l:

$$\Delta\zeta = -c\,(\mathbf{p}\cdot\mathbf{q})\,(\mathbf{E}\cdot\mathbf{q}) \bigg/ \left(\sigma^2 \sum_{j=1}^{N} \mathbf{p}^j\cdot\mathbf{p}^j\right). \quad (81)$$

Here, $c = \left(c^l - c^k\right)$ is the charge difference of the colliding particles. For collisions of particles with the same charge $\Delta\zeta$ vanishes and, consequently, the additional term $\delta\hat{\mathbf{p}}_f^j$ vanishes for noncolliding particles. For the momentum component belonging to the colliding particles we can write

$$\delta\hat{\mathbf{p}}_f^k = \left[c^k\mathbf{E}-\zeta(\mathbf{P}_i)\,\mathbf{p}_i^k - c^k\mathbf{E}+\zeta(\mathbf{P}_f)\,\mathbf{p}_f^k\right]\delta\tau_c + (c\mathbf{E}\cdot\mathbf{q})\,\mathbf{q}/\sigma^2\delta\tau_c, \quad (82)$$

$$\delta\hat{\mathbf{p}}_f^l = \left[c^l\mathbf{E}-\zeta(\mathbf{P}_i)\,\mathbf{p}_i^l - c^l\mathbf{E}+\zeta(\mathbf{P}_f)\,\mathbf{p}_f^l\right]\delta\tau_c - (c\mathbf{E}\cdot\mathbf{q})\,\mathbf{q}/\sigma^2\delta\tau_c, \quad (83)$$

which leads to

$$\delta\hat{\mathbf{p}}_f^k = \left[\Delta\zeta\mathbf{p}_i^k + (c\mathbf{E}\cdot\mathbf{q})\,\mathbf{q}/\sigma^2\right]\delta\tau_c, \quad (84)$$

$$\delta\hat{\mathbf{p}}_f^l = \left[\Delta\zeta\mathbf{p}_i^l - (c\mathbf{E}\cdot\mathbf{q})\,\mathbf{q}/\sigma^2\right]\delta\tau_c. \quad (85)$$

In summary, the total transformation rules for the color-conductivity system are given by

$$\delta\mathbf{q}_f^j = \delta\mathbf{q}_i^j \quad \text{for } j \neq k,l, \quad (86)$$

$$\delta\mathbf{q}_f^k = \delta\mathbf{q}_i^k + (\delta\mathbf{q}\cdot\mathbf{q})\,\mathbf{q}/\sigma^2, \quad (87)$$

$$\delta\mathbf{q}_f^l = \delta\mathbf{q}_i^l - (\delta\mathbf{q}\cdot\mathbf{q})\,\mathbf{q}/\sigma^2, \quad (88)$$

$$\delta\mathbf{p}_f^j = \delta\mathbf{p}_i^j + \Delta\zeta\mathbf{p}_i^j\delta\tau_c \quad \text{for } j \neq k,l, \quad (89)$$

$$\delta\mathbf{p}_f^k = \delta\mathbf{p}_i^k + (\delta\mathbf{p}\cdot\mathbf{q})\,\mathbf{q}/\sigma^2 + \frac{(\delta\mathbf{q}_i\cdot\mathbf{t}_i)}{\sigma\cos\alpha}|\mathbf{p}|\,\mathbf{t}_f + \left(\Delta\zeta\mathbf{p}_i^k + \frac{c}{\sigma^2}(\mathbf{E}\cdot\mathbf{q})\,\mathbf{q}\right)\delta\tau_c, \quad (90)$$

$$\delta\mathbf{p}_f^l = \delta\mathbf{p}_i^l - (\delta\mathbf{p}\cdot\mathbf{q})\,\mathbf{q}/\sigma^2 - \frac{(\delta\mathbf{q}_i\cdot\mathbf{t}_i)}{\sigma\cos\alpha}|\mathbf{p}|\,\mathbf{t}_f + \left(\Delta\zeta\mathbf{p}_i^l - \frac{c}{\sigma^2}(\mathbf{E}\cdot\mathbf{q})\,\mathbf{q}\right)\delta\tau_c. \quad (91)$$

We note that these rules obey $\delta K \equiv \sum(\delta\mathbf{p}^j\cdot\mathbf{p}^j)/m = 0$ as they should for the total kinetic energy to be conserved. Also $\delta\mathbf{Q} \equiv \sum\delta\mathbf{q}^j = \mathbf{0}$ and $\delta\mathbf{P} \equiv \sum\delta\mathbf{p}^j = \mathbf{0}$ hold as required by the conservation of the center-of-mass and linear momentum, respectively, provided that these conditions are fulfilled initially. We come back to this point in Sec. IV B.

It is worth mentioning that one may derive approximate algorithms by not taking the limit in Eq. (3) and treating $\delta\mathbf{\Gamma}(t)$ as a small but finite separation vector in phase space. We have used this method for checking our exact procedures outlined above, which treat $\delta\mathbf{\Gamma}(t)$ as a true tangent vector.

In the next section we describe the details and the results of our simulations for the two-dimensional hard-disk system in equilibrium and in nonequilibrium steady states.

IV. RESULTS

In all our numerical work we use reduced units for which the disk diameter σ, the disk mass m, and the Boltzmann constant k are equal to 1. The unit of time is $(m\sigma^2N/K)^{1/2}$, where K is the total kinetic energy. The density of the system is defined by $\rho = N/A$, where $A = L_xL_y$ is the area of the simulation cell, and L_x and L_y are the lengths of the simulation box in the x and y directions, respectively. We use periodic boundary conditions in both coordinate directions. In order to be able to simulate high density systems, we use a simulation box with an aspect ratio of $L_y/L_x = 2/\sqrt{3} \approx 1.1547$, which is compatible with the triangular close-packed lattice and deviates only slightly from a square shape. For the initial conditions the disk centers were located on a regular triangular lattice, and the momenta were chosen from a Gaussian distribution with zero mean and then adjusted to make the total momentum vanish. It suffices to consider a single isotherm for an unperturbed hard system. Since also Lyapunov exponents are proportional to $\sqrt{T}$, we restrict ourselves to the case $K = N$, i.e., the kinetic energy per particle is equal to 1. Thus, the only free parameter is the density ρ. For the temperature T the kinetic theory definition, $K = \sum\mathbf{p}^2/2m = (N-1)kT$, is used throughout.

As usual for the simulation of hard spheres we use a collision-by-collision approach. The collisions of the particles as well as the intersections with the simulation-box boundaries are treated exactly, so that our simulation results remain valid also for very low densities, since no collision event is missed.

A. Equilibrium systems

We computed full Lyapunov spectra for various densities and particle numbers. Since this requires the simultaneous integration of $4N(4N+1) \approx 16N^2$ equations of motion, we restrict ourselves to $N = 64$ and $N = 144$ particles corresponding to 256 and 576 exponents, respectively. These numbers are too small to allow a complete assessment of the thermodynamic limit, but suffice to give an overview of hard-disk Lyapunov spectra. Just as in the continuous case, we found that after a few collisions the Smale-pairing rule is obeyed exactly also for the local expansion and contraction rates of the offset vectors [24]. The computation of Lyapunov spectra for constrained continuously interacting particle systems has been discussed recently in Ref. [25].

Figures 3 and 4 show typical spectra for 64-disk and 144-disk systems, respectively, for the densities $\rho = 0.2\sigma^{-2}, 0.4\sigma^{-2}, 0.6\sigma^{-2}, 0.8\sigma^{-2}$, and $1.0\sigma^{-2}$. All spectra are normalized by their respective maximum exponents λ_1 listed in Table I. On the abscissa the index i enumerates conjugate pairs of exponents such that $i = 2N$ corresponds to the maximum and minimum exponents, $i = 2N-1$ to the next smaller and next larger exponents, and, finally, $i = 3$ to 1 refer to vanishing exponent pairs. Since the spectra in these figures belong to equilibrium systems, only the positive branches of the spectra are depicted. From the rate of convergence one can infer that the accuracy of the exponents presented in this and the

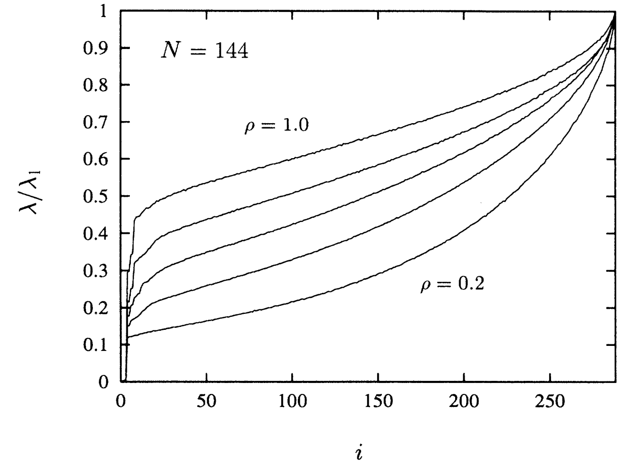

FIG. 4. Lyapunov spectra, normalized by the maximum exponent λ_1, for a system of 144 hard disks in equilibrium and for densities $\rho = 0.2\sigma^{-2}$, $0.4\sigma^{-2}$, $0.6\sigma^{-2}$, $0.8\sigma^{-2}$, and $1.0\sigma^{-2}$ (from bottom to top). The respective λ_1 is listed in Table I. The index i labels the Lyapunov exponents, which are defined only for integer i. For clarity a solid line is drawn through all exponent points. Only the positive branches of the spectra are depicted. The density $\rho = N/A$ is given in units of σ^{-2}, where σ is the disk diameter.

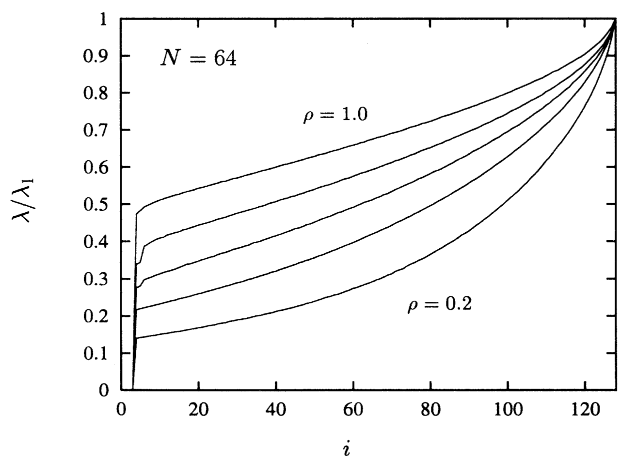

FIG. 3. Lyapunov spectra, normalized by the maximum exponent λ_1, for an equilibrium system of 64 hard disks and for densities $\rho = 0.2\sigma^{-2}$, $0.4\sigma^{-2}$, $0.6\sigma^{-2}$, $0.8\sigma^{-2}$, and $1.0\sigma^{-2}$ (from bottom to top). The respective λ_1 is listed in Table I. The index i labels the Lyapunov exponents, which are defined only for integer i. For clarity a solid line is drawn through all exponent points. Only the positive branches of the spectra are depicted. The density $\rho = N/A$ is given in units of σ^{-2}, where σ is the disk diameter.

TABLE I. Parameters characterizing the Lyapunov spectra for a system of N hard disks in equilibrium. ρ is the particle density in units of σ^{-2}. The collision rate $1/\tau$, the maximum Lyapunov exponent λ_1, the smallest positive Lyapunov exponent λ_{2N-4}, and the Kolmogorov-Sinai entropy per particle h_{KS}/N are all given in units of $(K/mN\sigma^2)^{1/2}$.

N	ρ	$1/\tau$	λ_{2N-4}	λ_1	h_{KS}/N
64	0.1	12.9	0.121	1.275	0.726
64	0.2	29.6	0.258	1.850	1.326
64	0.3	52.1	0.424	2.359	1.961
64	0.4	83.0	0.631	2.908	2.679
64	0.5	126.7	0.886	3.528	3.520
64	0.6	192.4	1.180	4.281	4.582
64	0.7	295.3	1.596	5.232	5.957
64	0.8	468.5	2.206	6.506	7.848
64	0.9	596.3	2.825	7.165	9.086
64	1.0	999.2	4.287	9.060	12.242
144	0.1	28.8	0.263	1.315	0.721
144	0.2	67.0	0.550	1.919	1.330
144	0.3	117.0	0.862	2.436	1.959
144	0.4	186.9	1.233	2.974	2.675
144	0.5	286.0	1.664	3.603	3.527
144	0.6	434.5	2.219	4.367	4.592
144	0.7	662.3	2.912	5.403	5.951
144	0.8	1052.6	3.857	6.664	7.843
144	0.9	1356.2	4.531	7.341	9.143
144	1.0	2258.0	6.132	9.252	12.296

subsequent figures is better than $\pm 0.5\%$. We find that all exponents grow with increasing density. One remarkable feature is that the smallest nonvanishing positive exponent λ_{2N-4} is rather large, quite different from the spectral shape found, for example, for Lennard-Jones liquids and solids [18,26], linear molecules [27], planar rotators [28], the Fermi-Pasta-Ulam (FPU) model [29], and even in products of random symplectic matrices [30], to mention only a few. All these systems, with the obvious exception of random matrices, have in common that their components interact with smooth potentials. We observe that for increasing density the spectra in Figs. 3 and 4 tend to become flatter. This is confirmed by Fig. 5, which depicts two normalized spectra at very low and very high densities. As the density approaches the close-packed density all Lyapunov exponents converge towards the same value.

Figure 6 shows the maximum and the smallest positive exponent, λ_1 and λ_{2N-4}, and the Kolmogorov-Sinai entropy per particle, h_{KS}/N, as a function of the density for a 64-disk system. The simulations include from 10^5 to 10^6 collisions depending on the density. This guarantees an accuracy better than 0.5% for all nonvanishing Lyapunov exponents shown. We have already mentioned before that λ_1 increases monotonically with density. It has a singularity at the close-packed density due to the divergence of the collision rate and converges towards zero in the limiting case of low densities. The same is true for h_{KS}, which, after Pesin [31], in Hamiltonian systems equals the sum of all positive Lyapunov exponents. It has been shown by Sinai that the entropy per particle of a hard-sphere gas converges towards a well defined value in the thermodynamic limit of $N \to \infty$ [32]. It is obvious from this figure that the density dependence of λ_1 and h_{KS} closely resembles that of the pressure calculated from the virial [33].

λ_1, λ_{2N-4}, and h_{KS} are also strongly affected by the phase transition occurring for densities $\rho \approx 0.86\sigma^{-2}$.

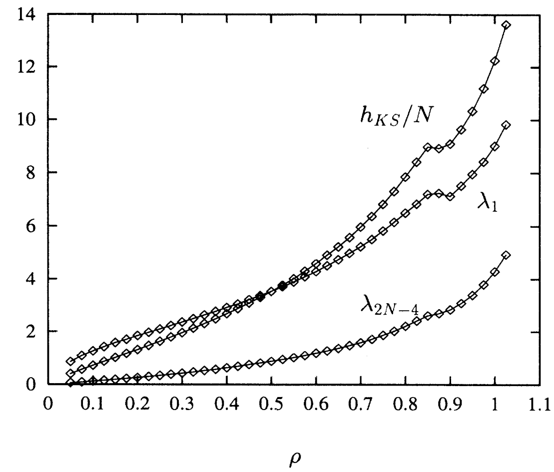

FIG. 6. Maximum Lyapunov exponent (λ_1), smallest positive exponent (λ_{2N-4}), and Kolmogorov-Sinai entropy h_{KS} per particle [all in units of $(K/mN\sigma^2)^{1/2}$] for the 64-disk system as functions of the density ρ (in units of σ^{-2}).

This can be attributed to the density dependence of the collision rate. In Fig. 7 the Kolmogorov-Sinai entropy per particle is shown as a function of the collision rate $1/\tau$, where τ is the collision time taken from the sumulations. Even for collision rates corresponding to the phase transition [$1/\tau \sim 600(K/Nm\sigma)^{1/2}$], no singularity appears, which proves our assertion. This is an important result since it provides the possibility of interpreting the mechanical instability in terms of the Enskog theory for hard-disk systems.

In order to determine the functional dependence of the maximum exponent in the low density limit we performed a series of simulations of a 64-disk system for densities ranging from $10^{-6}\sigma^{-2}$ to $10^{-1}\sigma^{-2}$. At the lowest density the mean free path exceeds $4\times 10^5\sigma$. In Fig. 8 λ_1 is plot-

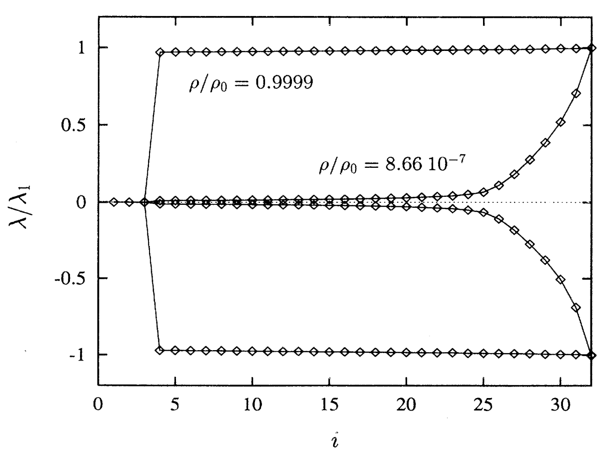

FIG. 5. Normalized Lyapunov spectrum of $N = 32$ hard disks at the densities $\rho/\rho_0 = 0.9999$ and $\rho/\rho_0 = 8.66 \times 10^{-7}$, where $\rho_0 = 1.1547\sigma^{-2}$ is the close-packed density.

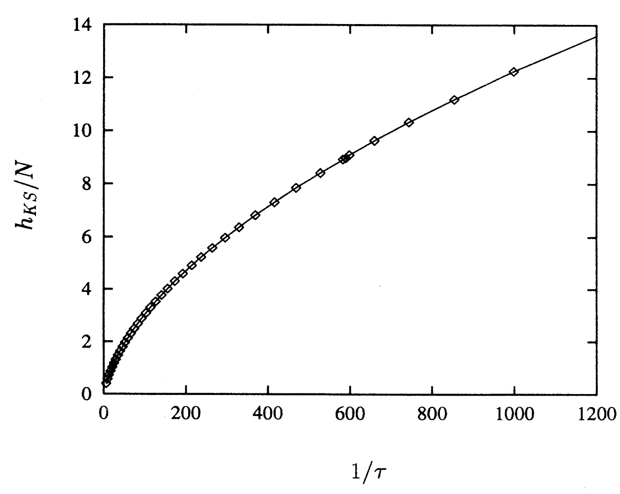

FIG. 7. Kolmogorov-Sinai entropy per particle as a function of the collision rate for the 64-disk system. Both h_{KS} and $1/\tau$ are given in units of $(K/mN\sigma^2)^{1/2}$.

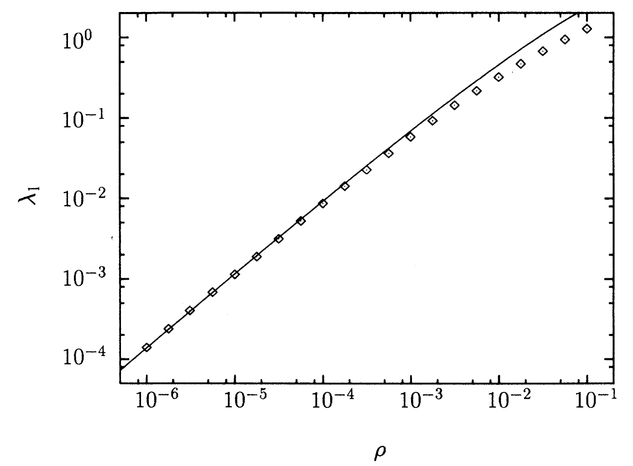

FIG. 8. Low density dependence of the maximum Lyapunov exponent λ_1 for a 64-disk system (diamonds). For each point at least 50 000 collisions were computed leading to an accuracy better than 1%. The smooth line is a fit of the Krylov relation $a\rho\ln(\rho/b)$ to the data points. ρ is given in units of σ^{-2}, and λ_1 is measured in units of $(K/Nm\sigma^2)^{1/2}$.

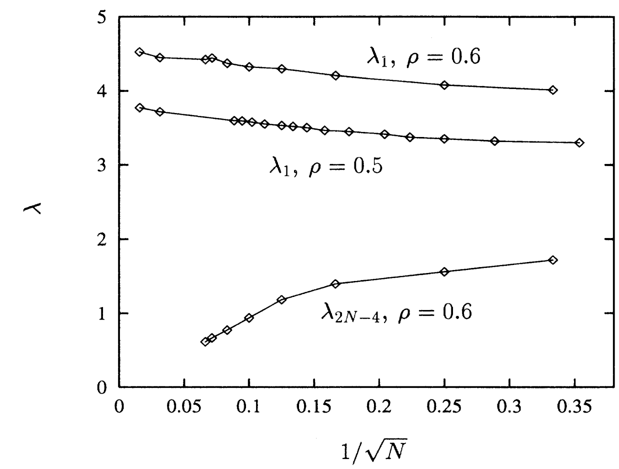

FIG. 9. Specified Lyapunov exponents as a function of $N^{-1/2}$ for various densities ρ. λ_1 is the maximum exponent and λ_{2N-4} the smallest positive exponent, both measured in units of $(K/mN\sigma^2)^{1/2}$. The density is given in units of σ^{-2}.

ted as a function of the density. The open symbols are the results of our simulations, whereas the line represents a fit of the relation $\lambda_1 \propto -\rho\ln\rho$ to our data. This relation was proposed by Krylov [34] by considering the angular divergence of trajectories starting from the same point in configuration space with momenta pointing in directions separated by small angle differences. Sinai [34] and Gaspard and Wang [35] discussed this relation in some detail. van Beijeren and Dorfman [36] derived it for the two-dimensional Lorentz gas by solving the Boltzmann-Lorentz equation and succeeded in determining the proportionality constant and the first correction.

There is numerical evidence that a thermodynamic limit exists for the Lyapunov spectrum. This has been emphasized by Livi, Politi, and Ruffo for the one-dimensional Fermi-Pasta-Ulam chain (β model) [29], and by Hoover and Posch, who computed the maximum exponent for two-dimensional nonequilibrium systems with Sllod (so named because of the close relationship with the Dolls tensor algorithm) equations of motion for particle numbers ranging from $N = 64$ to 32 400 [4]. Our numerical results are in agreement with these findings. Figure 9 shows the maximum exponent for densities $\rho = 0.5\sigma^{-2}$ and $\rho = 0.6\sigma^{-2}$ as a function of $1/\sqrt{N}$. λ_1 for $N = 4096$ is already close to its thermodynamic limit, whereas λ_{2N-4} seems to approach zero. However, a logarithmic singularity cannot be excluded. Figure 9 also suggests that the step in the spectra for small indices i does not persist in the thermodynamic limit and is therefore a peculiarity of small systems. We expect—but cannot prove—isochoric convergence to a thermodynamic-limit spectrum in accordance with theoretical expectation [37]. It is worth mentioning, however, that there is no thermodynamic limit for the root mean square displacement [38–40] in two dimensions.

B. Color conductivity of hard-disk systems in nonequilibrium steady states

Up to now, nonequilibrium phenomena involving hard particles have been mainly investigated for a two-particle system in two dimensions. In this so-called Lorentz gas shear viscosities and conductivities have been calculated by nonequilibrium molecular dynamics [20–22,41,42]. For heat conduction, which has also been studied [43], at least three hard disks are required. In this section we present the results of our simulations of many-body hard-disk systems subjected to an external color field. This model is described in detail in Sec. III E, where also the algorithm for the computation of Lyapunov exponents is derived.

We use the same periodic boundaries and initial conditions as in the equilibrium case. The particles are alternately assigned the color charges $+1$ and -1. For an even number of particles charge neutrality is automatically achieved, which is required for the conservation of total momentum. For an odd number of particles fractional charges are used to fulfill this requirement.

In contrast to the equilibrium case no analytical solution for the intercollisional trajectory is available, and the equations of motion in phase space and in tangent space are integrated numerically. We use a fourth-order Runge-Kutta integrator [44] with a time step of $\Delta t = 0.01(m\sigma^2N/K)^{1/2}$. This assures that the relative kinetic energy fluctuations are below 10^{-7}. The coordinates of two colliding disks are numerically determined with an accuracy of $10^{-6}\sigma$ and the respective collision rules derived in Sec. III E are applied to the phase space vector and the tangent space offset vectors. This error level is perfectly adequate for the desired accuracy of the resulting Lyapunov exponents.

The disks moving under the influence of the external perturbation continually extract energy from the field and must therefore be thermostatted to achieve a steady state. The system is dissipative and the phase space distribution collapses onto a multifractal strange attractor with information dimension less than the phase space dimension. Since the collisions conserve phase volume, shrinking takes place only in the intercollisional trajectory segments and is obtained from the phase space divergence of equations of motion (74)–(76):

$$\langle \nabla_{\mathbf{\Gamma}} \cdot \dot{\mathbf{\Gamma}} \rangle = \sum_{l=1}^{4N} \lambda_l = -(2N-1)\langle \zeta \rangle. \tag{92}$$

This equation holds if the offset-vector dynamics is followed in the full $4N$-dimensional phase space and no explicit constraints following from momentum conservation are invoked (see the discussion at the end of this section). Since the time average of the phase space divergence is equal to the sum of the Lyapunov exponents and $\langle \zeta \rangle$ is positive, the sum of the Lyapunov exponents is negative. The Smale pairing is replaced by the conjugate pairing rule [6,45]

$$\lambda_l + \lambda_{4N+1-l} = -\langle \zeta \rangle. \tag{93}$$

According to (76) the thermostat variable is given by

$$\zeta = (\mathbf{J} \cdot \mathbf{E})/2K, \tag{94}$$

where $\mathbf{J} = \sum_i c^i \mathbf{p}^i / m$ is the total color current of the system [18,26]. We define the field-dependent nonlinear conductivity by $\kappa = j/|\mathbf{E}|$, where $j = \langle \mathbf{J} \cdot \mathbf{E} \rangle / N|\mathbf{E}|$ is the average current per particle in the field direction.

1. Systems with 64 hard disks

In Fig. 10 typical Lyapunov spectra of a 64-particle system for the densities $\rho = 0.4\sigma^{-2}, 0.6\sigma^{-2}$ and $0.8\sigma^{-2}$ are shown. The labels a, b, and c refer to the strength of the field pointing in the x direction. For low fields (curve a) the steplike shape typical for hard disks is still observed for small indices i. For higher fields (curves b and c) this step is gradually smoothed out. We note that the small exponents are affected most by the external perturbation. In addition, due to the action of the field the whole spectrum is shifted towards more negative values in accordance with the pairing rule. This shift is obvious from the solid horizontal lines in the figures which connect the arithmetic means for the respective conjugate pairs of Lyapunov exponents. For a given field the arithmetic mean decreases with increasing density.

A series of simulations was performed to study the field dependence of the maximum Lyapunov exponent as a function of the field strength, where the field vector pointed in the x direction parallel to one side of the simulation box. Figure 11 shows that for large densities ($\rho = 0.8\sigma^{-2}$) the maximum exponent λ_1 is nearly constant over the whole range of fields, whereas it decreases slowly with increasing field for lower densities

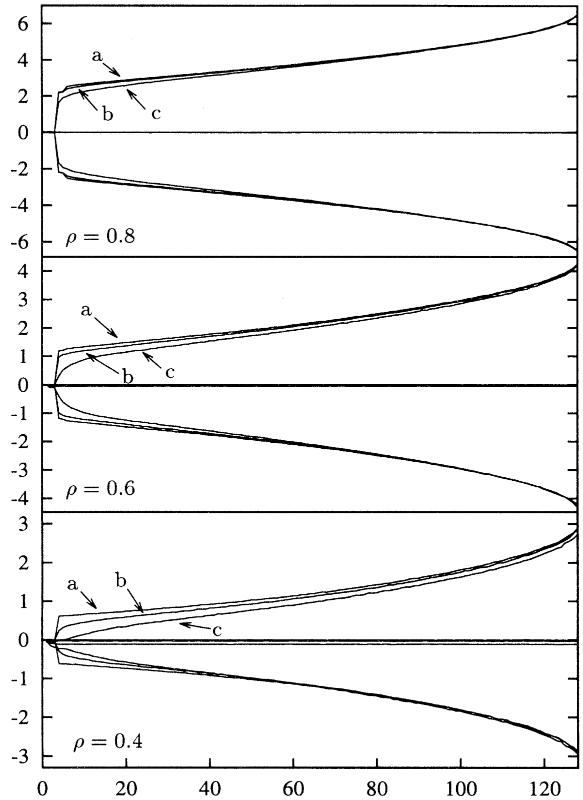

FIG. 10. Full Lyapunov spectra of a 64-disk system for the densities $\rho = 0.4\sigma^{-2}$ (top), $\rho = 0.6\sigma^{-2}$ (middle), and $\rho = 0.8\sigma^{-2}$ (bottom). The labels a–c refer to the applied color field: a: $\mathbf{E} = (0.1, 0.0)K/N\sigma$; b: $\mathbf{E} = (0.5, 0.0)K/N\sigma$; and c: $\mathbf{E} = (1.0, 0.0)K/N\sigma$. The field always points in the x direction. On the abscissa the exponent pairs are numbered by an index i. They are defined only for integer i; for clarity the points are connected by a solid line. The arithmetic mean of conjugate Lyapunov exponent pairs is also indicated by the solid horizontal lines, which differ significantly and visibly from zero for $\rho = 0.4\sigma^{-2}$ and for the largest field. All exponents are measured in units of $(K/Nm\sigma^2)^{1/2}$.

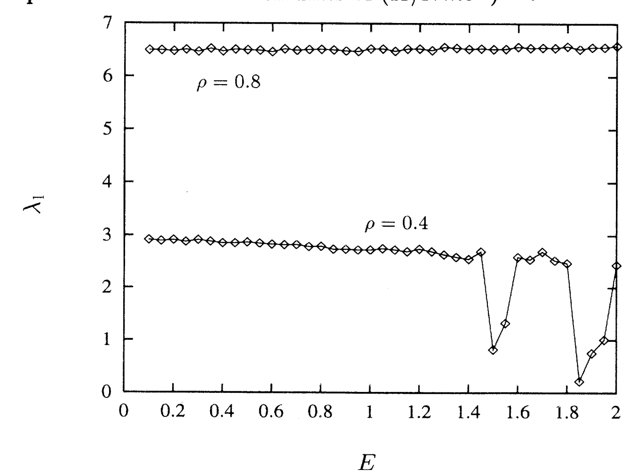

FIG. 11. Maximum Lyapunov exponent of a 64-disk color-conductivity model for the densities $\rho = 0.4\sigma^{-2}$ and $\rho = 0.8\sigma^{-2}$ as a function of the field strength. The field vector points in the x direction and is measured in units of $K/N\sigma$.

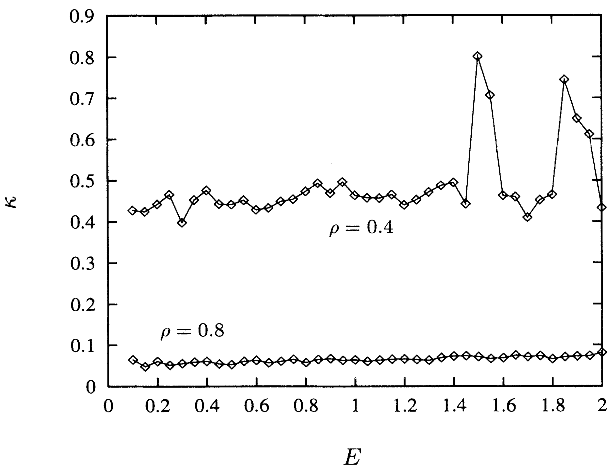

FIG. 12. Field dependence of the color conductivity of a 64-disk system for the densities $\rho = 0.4\sigma^{-2}$ and $\rho = 0.8\sigma^{-2}$. The conductivity is measured in units of $(\sigma^2 N/Km)^{1/2}$, and the field in units of $K/N\sigma$.

$(\rho = 0.4\sigma^{-2})$.

At higher fields the system can be trapped in nonergodic trajectories, where the particles drift past each other without collisions. The probability of such states increases with higher fields. The irregular behavior of λ_1 for strong fields in Fig. 11 means that the system has reached such an ordered state characterized by small or vanishing Lyapunov exponents, and that λ_1 has not yet converged in spite of a long simulation run. This irregularity is visible also in Fig. 12, which shows the conductivity as a function of the field strength. κ is only weakly dependent on $\mathbf{E}$ except for these singular states.

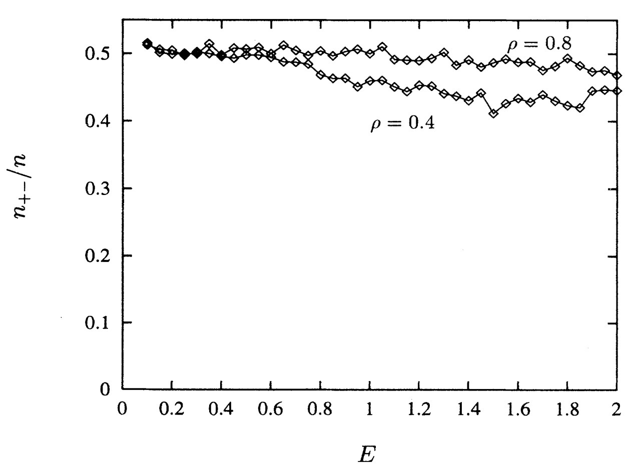

FIG. 13. Fraction of collisions between particles carrying opposite charges for a 64-disk color-conductivity model at the densities $\rho = 0.4\sigma^{-2}$ and $\rho = 0.8\sigma^{-2}$ as a function of the field strength. The field points in the x direction and is measured in units of $K/N\sigma$.

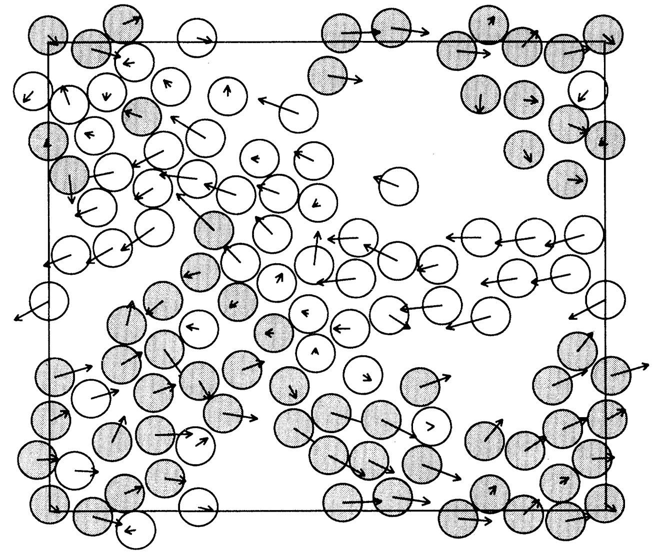

FIG. 14. Snapshot of a typical nonequilibrium steady-state configuration of a 100-disk color-conductivity system at a density of $\rho = 0.6\sigma^{-2}$. The color field $\mathbf{E} = (2,0)\,K/N\sigma$ points in the x direction. The instantaneous particle velocity is indicated by the arrows.

Of course, for these states the current is bounded only by the action of the thermostat, which results in a high conductivity. Except for this singular behavior the conductivity decreases with increasing density, as expected.

If the system is driven at high enough dissipation rates, an interesting demixing instability occurs as was observed by Evans, Lynden-Bell, and Morriss [46]. In contradiction to intuition the fraction of collisions between disks carrying opposite color charges decreases with increasing field strength as may be seen in Fig. 13. This behavior is explained, however, by Fig. 14, which shows a typical steady-state configuration of a 100-particle system at a density of $0.6\sigma^{-2}$ and with a field $\mathbf{E} = (2,0)\,(mK/N)^{1/2}$ in the x direction. One observes the formation of clusters of particles with the same color charge. The clusters are not stable, but are continuously formed and disrupted again. Since a particle belonging to a cluster is more likely to collide with one of the surrounding disks carrying the same color charge, the fraction of collisions of particles with opposite charges decreases.

2. Systems with three and four hard disks

The conjugate pairing rule (93) has been rigorously proved only in the limit $N \to \infty$ when corrections of $O\,(1/N)$ can be neglected [6,17,45,47]. In order to check whether or not an N dependence may be observed and a pairing rule exists for systems with only a few particles, we performed a series of color-conductivity simulations with $N = 3$ and $N = 4$ particles. For $N = 3$ two disks carry a color charge $c = 2/3$ and one a charge $c = -4/3$

such that the total color charge vanishes. If the density of the system is low and the driving field strong, the system is observed to converge towards a limit cycle after a few collisions on which the disks drift collision-free in the field direction. A similar phenomenon was responsible for the singular behavior at large fields for the 64-disk simulations of Figs. 12 and 13. In order to avoid such nonergodic trajectories characterized by a Lyapunov spectrum without positive exponents, we choose a field direction which is not parallel to one side of the simulation box. This ensures that, due to the periodic boundaries, a disk traveling in the field direction necessarily collides with a disk carrying an opposite charge.

Figures 15 and 16 show the results of these three- and four-particle simulations, where Lyapunov spectra are depicted for a density of $\rho = 0.5\sigma^{-2}$ and for the field components indicated by the labels. For clarity the various exponents belonging to one spectrum and defined only for integer i are connected by solid lines. For each conjugate pair of exponents their arithmetic mean $(\lambda_l + \lambda_{4N+1-l})/2$ is also connected by the dashed horizontal lines. The respective conductivities κ, the time averaged thermostat variables $\langle\zeta\rangle$, and the maximum Lyapunov exponents λ_1 for these runs are listed in Table II.

Let us discuss the three-particle case in more detail. The spectra in Fig. 15 were obtained by performing the simulation in the *full 12-dimensional* phase and tangent spaces *without explicit consideration* of the natural constants of the motion—kinetic energy, linear momentum, and center of mass. (It should be noted that due to the periodic boundaries the center of mass is not literally conserved. But since this does not affect the dynamics in tangent space each component of the center of mass still causes one of the Lyapunov exponents to vanish.) There are altogether 12 exponents for each spectrum arranged in such an order that the conjugate pair λ_1, λ_{12} is located at index $i = 6$, the pair λ_2, λ_{11} at $i = 5$, and, finally, the two vanishing exponents, λ_6 and λ_7, at $i = 1$. In view of the five constants of the motion and the vanishing exponent in the direction of the phase flux one expects six of the exponents to vanish. However, an inspection of Fig. 15 reveals that there are only *four vanishing exponents*, λ_4–λ_7, with two further exponents $\lambda_8 = \lambda_9 = -\langle\zeta\rangle < 0$. The reason for this discrepancy is clarified if one realizes that the quantities

$$\sum_{j=1}^{N} \mathbf{q}^j = \mathbf{0}, \quad \sum_{j=1}^{N} \mathbf{p}^j = \mathbf{0}, \quad \sum_{j=1}^{N} \mathbf{p}^{j2}/2m = K \tag{95}$$

are constants of the motion for a charge-neutral system with vanishing total momentum. Then the respective components of the tangent vectors obey

$$\sum_{j=1}^{N} \delta\mathbf{q}^j \equiv \delta\mathbf{Q} = \mathbf{0}, \quad \sum_{j=1}^{N} \delta\mathbf{p}^j \equiv \delta\mathbf{P} = \mathbf{0},$$

$$\sum_{j=1}^{N} (\mathbf{p}^j \cdot \delta\mathbf{p}^j)/m \equiv \delta K = 0. \tag{96}$$

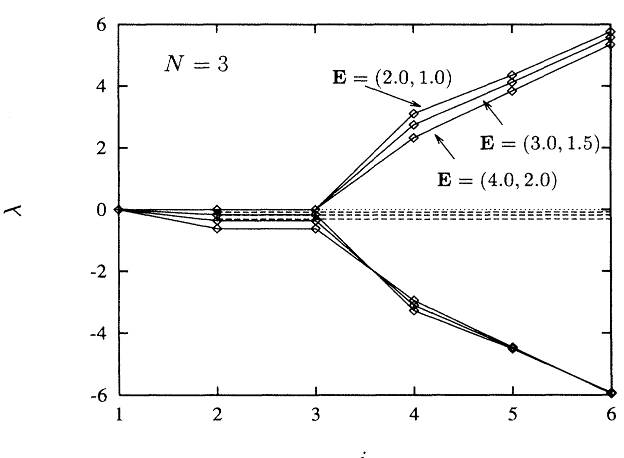

FIG. 15. Lyapunov spectra of a three-disk color-conductivity system in nonequilibrium steady states specified by the density $\rho = 0.6\sigma^{-2}$ and the fields indicated by the labels. The field components are given in units of $K/N\sigma$. Only the magnitude of the field is varied, its direction is kept fixed. Six pairs of conjugate Lyapunov exponents are arranged according to an index i along the abscissa. Points denoting the arithmetic means of conjugate Lyapunov exponent pairs are connected by dashed lines. The Lyapunov exponents are measured in units of $(K/Nm\sigma^2)^{1/2}$. For details we refer to the main text.

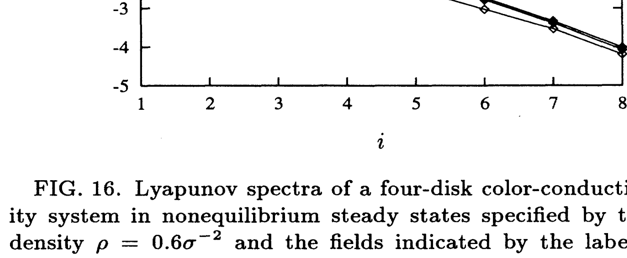

FIG. 16. Lyapunov spectra of a four-disk color-conductivity system in nonequilibrium steady states specified by the density $\rho = 0.6\sigma^{-2}$ and the fields indicated by the labels. The field components are given in units of $K/N\sigma$. Only the magnitude of the field is varied; its direction is kept fixed. Eight pairs of conjugate Lyapunov exponents are arranged according to an index i along the abscissa. Points denoting the arithmetic means of conjugate Lyapunov exponent pairs are connected by dashed lines. The Lyapunov exponents are measured in units of $(K/Nm\sigma^2)^{1/2}$. For details we refer to the main text.

TABLE II. Parameters characterizing a planar nonequilibrium steady-state system of $N = 3$ and $N = 4$ disks subjected to an external color field $\mathbf{E} = (E_x, E_y)$. The field components are given in units of $K/N\sigma$. The color conductivity κ is given in units of $(\sigma^2 N/Km)^{1/2}$, the time averaged thermostat variable $\langle\zeta\rangle$ and the maximum Lyapunov exponent λ_1 in units of $(K/Nm\sigma^2)^{1/2}$.

N	$\mathbf{E}$	κ	$\langle\zeta\rangle$	λ_1
3	(2.0, 1.0)	0.066	0.16513	5.758
3	(3.0, 1.5)	0.063	0.35874	5.575
3	(4.0, 2.0)	0.061	0.61925	5.341
4	(2.0, 1.0)	0.102	0.25624	3.752
4	(3.0, 1.5)	0.126	0.71392	3.359
4	(4.0, 2.0)	0.173	1.73552	2.458

Each of these five constraints constitutes a hyperplane in tangent space. If one follows the dynamics of $4N$ orthonormal offset vectors in the full $4N$-dimensional tangent space there is necessarily one of these vectors perpendicular to this constraint plane, thus violating the respective constraint. It was noted at the end of Sec. III E that the quantities $\delta\mathbf{Q}$, $\delta\mathbf{P}$, and δK are not affected by the hard-core collision map. However, for the streaming between collisions we find from the linearized equations of motion (78)

$$\delta\dot{\mathbf{Q}} = \mathbf{0}, \quad \delta\dot{\mathbf{P}} = -\zeta\delta\mathbf{P}, \quad \delta\dot{K} = 0. \tag{97}$$

It follows that offset-vector components perpendicular to the center-of-mass and energy hyperplanes in tangent space do not change at all in the course of time and consequently contribute three vanishing Lyapunov exponents to the spectrum. The two vector components normal to the two hyperplanes associated with linear momentum conservation, however, shrink and lead to the two negative exponents $\lambda_8 = \lambda_9 = -\langle\zeta\rangle < 0$ for the case $N = 3$.

As suggested in [25] the dynamics can be followed also in the *reduced phase space* of the first $N - 1$ particles by expressing $\mathbf{q}_N$, $\mathbf{p}_N$, $\delta\mathbf{q}_N$, and $\delta\mathbf{p}_N$ in terms of the respective negative sums of the remaining $N - 1$ particles. There are, of course, $4(N-1)$ Lyapunov exponents in this case, of which two vanish due to energy conservation and the phase flux direction. We have experimentally verified that the Lyapunov spectra obtained with both methods are identical except for the four exponents missing in the reduced phase space description: two vanishing exponents due to center-of-mass conservation (λ_4 and λ_5 for $N = 3$ in Fig. 15), and two exponents equal to $-\langle\zeta\rangle$ associated with this subtle violation of the momentum-conservation constraint in tangent space (λ_8 and λ_9 for $N = 3$). Furthermore, in the reduced phase space description the expression for the phase space divergence (92) must be replaced by

$$\langle \nabla_{\Gamma^{\mathrm{red}}} \cdot \dot{\Gamma}^{\mathrm{red}} \rangle = \sum_{l=1}^{4(N-1)} \lambda_l = -(2N-3)\langle\zeta\rangle. \tag{98}$$

The case of $N = 4$ particles in Fig. 16 is completely analogous and need not be discussed any further. It is also obvious that a system of only $N = 2$ particles has only one nontrivial conjugate pair of nonvanishing exponents and is therefore unsuited for a test of the conjugate pairing rule.

All spectra in Figs. 15 and 16 are for the same density $\rho = 0.5\sigma^{-2}$. The external field is indicated by the labels. It varies only in magnitude but not in direction. Each run was followed for 5×10^7 time steps corresponding to 1.6×10^6 collisions for the three-disk system, and to 1.8×10^6 collisions in the four-disk case. In these figures all points denoting the arithmetic means of nonvanishing conjugate pairs of the various spectra are connected by dashed lines. A close inspection of these results reveals that any possible deviation from an exact pairing rule—if it exists at all—is very small. To make this statement more precise we have listed in Table III the conjugate pair sums $\lambda_l + \lambda_{4N+1-l}$, $l = 1, 2, \ldots, 2N - 1$, for various spectra obtained with $N = 2$ and $N = 3$ particles. Their maximum relative deviation is less than 0.1% in all cases. The pair sums also agree extremely well with $-\langle\zeta\rangle$ listed in Table II—as required by Eq. (93) for the conjugate pairing rule to hold.

Tiny numerical deviations of a few pair sums from their mean may be noticed in Table III, but only for the largest applied color fields and still smaller than the accuracy

TABLE III. Sums of conjugate Lyapunov exponent pairs $\lambda_l + \lambda_{4N+1-l}$ for a stationary nonequilibrium color-conductivity simulation of a planar hard-disk system containing $N = 2$ or $N = 3$ disks. l denotes the exponent pair ($l = 1$ refers to the sum $\lambda_1 + \lambda_{4N}$ of the maximum and the minimum exponents). The components of the color field $\mathbf{E} = (E_x, E_y)$ are given in units of $K/N\sigma$ and the Lyapunov exponent sums in units of $(K/mN\sigma^2)^{1/2}$.

l	$N = 3$			$N = 4$		
	$\mathbf{E} = (2, 1)$	$\mathbf{E} = (3, 1.5)$	$\mathbf{E} = (4, 2)$	$\mathbf{E} = (2, 1)$	$\mathbf{E} = (3, 1.5)$	$\mathbf{E} = (4, 2)$
1	-0.16518	-0.35871	-0.61916	-0.25622	-0.71394	-1.7355
2	-0.16518	-0.35873	-0.61916	-0.25622	-0.71394	-1.7355
3	-0.16518	-0.35873	-0.61916	-0.25625	-0.71394	-1.7355
4	-0.16517	-0.35869	-0.61910	-0.25623	-0.71393	-1.7355
5	-0.16518	-0.35872	-0.61916	-0.25622	-0.71396	-1.7347
6				-0.25622	-0.71390	-1.7339
7				-0.25623	-0.71394	-1.7355

claimed in this paper. Work is in progress for a further reduction of the error bars.

We conclude that the conjugate pairing principle is numerically confirmed to within an accuracy of better than 0.1% for our systems as small as three and four particles.

V. SUMMARY

In this paper we have presented a method for the calculation of full Lyapunov spectra in systems for which the smooth phase space flux is interrupted by a differentiable map at discrete times. We derived the exact transformation rules for the tangent space offset vectors for systems of hard spheres in equilibrium and in nonequilibrium steady states.

Full Lyapunov spectra were obtained for a whole range of densities ρ and particle numbers N. For small particle numbers ($N \leq 64$) the spectra display an interesting steplike shape, which is smoothed out for larger N and does not seem to persist in the thermodynamic limit. From the positive branch of the Lyapunov spectrum the Kolmogorov-Sinai (KS) entropy was calculated. In the density regime of the fluid-solid phase transition the KS entropy is found to have a local maximum. As the density approaches the close-packed density the KS entropy as well as the maximum Lyapunov exponent diverge due to the singularity of the collision rate. For low densities the maximum Lyapunov exponents behaves as $-\rho \ln \rho$, as conjectured by Krylov on the basis of a mechanical stability argument [34,48,49].

In the steady nonequilibrium case with a color current in the direction of an external field, full Lyapunov spectra were calculated for various densities and field strengths both for large (64 disks) and for very small systems (three and four disks). The steplike shape of the spectra, typical for hard disks in equilibrium, is smoothed out by the action of the external perturbation. Simulations for the few-particle systems reveal that the conjugate pairing rule is obeyed. The numerical accuracy for the sums of conjugate exponent pairs used for this test is better than 0.1%. This result is quite remarkable in view of the fact that the the Lyapunov exponents are global properties of the system, and that the conjugate pairing principle need not necessarily be obeyed locally but only in the long time limit. Furthermore, the analytical proof of this principle relies on the assumption that quantities of the order $O(1/N)$ can be neglected.

ACKNOWLEDGMENTS

The authors gratefully acknowledge financial support from the Fonds zur Förderung der wissenschaftlichen Forschung, Grant No. P09677, and the generous allocation of computer resources by the Computer Center of the University of Vienna. Work in Livermore was performed under the auspices of the United States Department of Energy at the Lawrence Livermore National Laboratory under Contract No. W-7405-Eng-48.

[1] B. J. Alder and T. E. Wainwright, J. Chem. Phys. **33**, 1439 (1960).
[2] B. J. Alder and T. E. Wainwright, J. Chem. Phys. **31**, 459 (1959).
[3] B. J. Alder, in *Molecular Dynamics Simulations of Statistical-Mechanical Systems*, Proceedings of the International School of Physics "Enrico Fermi," Course XCVII, Varenna, 1985, edited by G. Ciccotti and W. G. Hoover (North-Holland, Amsterdam, 1986).
[4] W. G. Hoover and H. A. Posch, Phys. Rev. E **51**, 273 (1995).
[5] H. A. Posch and W. G. Hoover, in *Molecular Liquids: New Perspectives in Physics and Chemistry*, Vol. 379 of *NATO Advanced Study Institute, Series C*, edited by J. J. C. Teixeira-Dias (Kluwer Academic, Dordrecht, 1992), p. 527.
[6] D. J. Evans, E. G. D. Cohen, and G. P. Morriss, Phys. Rev. A **42**, 5990 (1990)
[7] B. J. Alder and T. E. Wainwright, Phys. Rev. **127**, 359 (1962).
[8] B. J. Alder and T. E. Wainwright, J. Chem. Phys. **27**, 1208 (1957).
[9] D. V. Anosov and Ya. G. Sinai, Russ. Math. Surv. **22**, 103 (1967).
[10] Ya. G. Sinai, Russ. Math. Surv. **25**, 137 (1970).
[11] V. I. Arnold and A. Avez, *Ergodic Problems of Classical Mechanics* (Benjamin, New York, 1968).
[12] W. G. Hoover, *Computational Statistical Mechanics* (Elsevier, Amsterdam, 1991).
[13] G. Benettin, L. Galgani, A. Giorgilli, and J.-M. Strelcyn, Meccanica **15**, 9 (1980).
[14] A. Wolf, J. B. Swift, H. L. Swinney, and J. A. Vastano, Physica D **16**, 285 (1985).
[15] W. G. Hoover and H. A. Posch, Phys. Rev. E **49**, 1913 (1994).
[16] V. I. Oseledec, Trans. Moscow Math. Soc. **19**, 197 (1968).
[17] S. Sarman, D. J. Evans, and G. P. Morriss, Phys. Rev. A **45**, 2233 (1992).
[18] H. A. Posch and W. G. Hoover, Phys. Rev. A **38**, 473 (1988).
[19] Ch. Dellago and H. A. Posch, Phys. Rev. E. **52**, 2401 (1995).
[20] Ch. Dellago, L. Glatz, and H. A. Posch, Phys. Rev. E **52**, 4817 (1995).
[21] J. Lloyd, M. Niemeyer, L. Rondoni, and G. P. Morriss, Chaos **5**, 536 (1995).
[22] B. Moran and W. G. Hoover, J. Stat. Phys. **48**, 709 (1987).
[23] D. J. Evans, W. G. Hoover, B. H. Failor, B. Moran, and A. J. C. Ladd, Phys. Rev. A **28**, 1016 (1983).
[24] W. G. Hoover, C. G. Hoover, and H. A. Posch, Phys. Rev. A **41**, 2999 (1990).
[25] W. G. Hoover, H. A. Posch, and L. W. Campbell, Chaos **3**, 325 (1993).

[26] H. A. Posch, W. G. Hoover, and B. L. Holian, Ber. Bunsenges. Phys. Chem. **94**, 250 (1990).
[27] I. Borszak, A. Baranyai, and H. A. Posch (unpublished).
[28] Ch. Dellago and H. A. Posch (unpublished).
[29] R. Livi, A. Politi, and S. Ruffo, J. Stat. Phys. **19**, 2033 (1986).
[30] G. Paladin and A. Vulpiani, J. Phys. A **19**, 1881 (1986).
[31] Ja. B. Pesin, Sov. Math. Dokl. **17**, 196 (1976).
[32] Ya. G. Sinai and N. I. Chernov, in *Dynamical Systems*, edited by Ya. G. Sinai (World Scientific, Singapore, 1991), p. 373.
[33] W. G. Hoover and B. J. Alder, J. Chem. Phys. **46**, 686 (1966).
[34] N. S. Krylov, in *Works on the Foundations of Statistical Mechanics*, edited by A. S. Wightman and P. W. Anderson (Princeton University Press, Princeton, 1979); Ya. G. Sinai, *ibid.*, p. 239.
[35] P. Gaspard and X.-J. Wang, Phys. Rep. **235**, 291 (1993).
[36] H. van Beijeren and J. R. Dorfman, Phys. Rev. Lett. **74**, 1319 (1995).
[37] Ya. G. Sinai (unpublished).
[38] W. G. Hoover, W. T. Ashurst, and R. J. Olness, J. Chem. Phys. **60**, 4043 (1974).
[39] H. A. Posch and W. G. Hoover, Phys. Rev. A **39**, 2175 (1989).
[40] W. G. Hoover and O. Kum, J. Chem. Phys. **103**, 1718 (1995).
[41] J. Petravic, D. J. Isbister, and G. P. Morris, J. Stat. Phys. **76**, 1045 (1994).
[42] W. G. Hoover, C. G. Hoover, W. J. Evans, B. Moran, J. A. Levatin, and E. A. Craig, in *Microscopic Simulations of Complex Flows*, Vol. 236 of *NATO Advanced Study Institute, Series B: Physics*, edited by M. Mareshal (Plenum, New York, 1990), p. 199.
[43] W. G. Hoover and K. W. Kratky, J. Stat. Phys. **42**, 1103 (1986).
[44] F. J. Vesely, *Computational Physics, An Introduction* (Plenum Press, New York, 1994).
[45] D. Gupalo, A. S. Kaganovich, and E. G. D. Cohen, J. Stat. Phys. **74**, 1145 (1994).
[46] D. J. Evans, R. M. Lynden-Bell, and G. P. Morriss, Mol. Phys. **67**, 209 (1989).
[47] E. G. D. Cohen, Physica A **213**, 293 (1995).
[48] S. D. Stoddard and J. Ford, Phys. Rev. A **8**, 1504 (1973).
[49] P. Gaspard and J. R. Dorfman, Phys. Rev. E. **52**, 3525 (1995).